Indicator minerals in fine-fraction till heavy-mineral concentrates determined by automated mineral analysis: examples from two Canadian polymetallic base-metal deposits

H.D. Lougheed[1*], M.B. McClenaghan[2], D. Layton-Matthews[1], and M.I. Leybourne[1,3]

Lougheed, H.D., McClenaghan, M.B., Layton-Matthews, D., and Leybourne, M.I., 2022. Indicator minerals in fine-fraction till heavy-mineral concentrates determined by automated mineral analysis: examples from two Canadian polymetallic base-metal deposits; in *Targeted Geoscience Initiative 5: volcanic- and sediment-hosted massive-sulfide deposit genesis and exploration methods, (ed.) J.M. Peter and M.G. Gadd; Geological Survey of Canada, Bulletin 617, p. 247–286. https://doi.org/10.4095/328011*

Abstract: Exploration under glacial sediment cover is a necessary part of modern mineral exploration in Canada. Traditional indicator methods use visual examination to identify mineral grains in the 250 to 2000 µm fraction of till heavy-mineral concentrates (HMC). This study tests automated mineralogical methods using scanning electron microscopy to identify indicator minerals in the fine (<250 µm) HMC fraction of till. Automated mineralogy of polished grains from the fine HMC enables rapid data collection (10 000–300 000 grains/sample). Samples collected near two deposits were used to test this method: four from the upper-amphibolite facies Izok Lake volcanogenic massive-sulfide deposit, Nunavut, and five from the Sisson granite-hosted W-Mo deposit, New Brunswick.

The less than 250 µm HMC fraction of till samples collected down ice of each deposit contain ore and alteration minerals typical of their deposit type. Sulfide minerals occur mainly as inclusions in oxidation-resistant minerals, including minerals previously identified in each deposit's metamorphic alteration halo, and are found to occur farther down ice than the grains identified visually in the greater than 250 µm HMC fraction. This project's workflow expands the detectable footprint for certain indicator minerals and enhances the information that can be collected from till samples.

Résumé : L'exploration de terrains enfouis sous une couverture de sédiments glaciaires est un aspect essentiel de l'exploration minérale moderne au Canada. Les méthodes de minéraux indicateurs classiques sont fondées sur un examen visuel visant à identifier les grains minéraux dans la fraction de 250 à 2 000 µm des concentrés de minéraux lourds (CML) du till. Dans la présente étude, nous avons mis à l'essai des méthodes minéralogiques automatisées ayant recours à la microscopie électronique à balayage pour identifier les minéraux indicateurs dans la fraction fine (<250 µm) des CML du till. La détermination automatisée de la minéralogie des grains polis des CML permet une collecte rapide de données (de 10 000 à 300 000 grains/échantillon). Pour mettre à l'essai cette méthode, nous avons utilisé des échantillons prélevés à proximité de deux gisements : quatre échantillons proviennent du gisement d'Izok Lake, au Nunavut, un gîte de sulfures massifs volcanogènes métamorphisé au faciès des amphibolites supérieur, et cinq échantillons, du gisement de Sisson, au Nouveau-Brunswick, un gîte de W-Mo encaissé dans un granite.

La fraction des CML inférieure à 250 µm dans les échantillons de till prélevés en aval glaciaire de chaque gisement contient des minéraux métallifères et des minéraux d'altération représentatifs de leur type de gîte. Les minéraux sulfurés se présentent principalement sous forme d'inclusions dans des minéraux résistant à l'oxydation, dont des minéraux précédemment identifiés dans l'auréole d'altération métamorphique de chaque gisement, et peuvent être trouvés plus loin en aval glaciaire que les grains identifiés visuellement dans la fraction de plus de 250 µm des CML. Le flux de travail de ce projet permet d'élargir l'empreinte détectable de certains minéraux indicateurs et d'améliorer l'information que l'on peut tirer des échantillons de till.

[1]Queen's Facility for Isotope Research, Department of Geological Sciences and Geological Engineering, Queen's University, 6 Union Street, Kingston, Ontario K7L 3N6
[2]Geological Survey of Canada, 601 Booth Street, Ottawa, Ontario K1A 0E8
[3]McDonald Institute, Canadian Particle Astrophysics Research Centre, Department of Physics, Engineering Physics & Astronomy, Queen's University, 64 Bader Lane, Kingston, Ontario K7L 3N6
*Corresponding author: H.D. Lougheed (email: 5hdl@queensu.ca)

INTRODUCTION

Indicator mineral methods applied to sediment samples are important exploration tools for diamonds (McClenaghan and Kjarsgaard, 2007) and gold (Averill and Zimmerman, 1986; Averill, 2001, 2013, 2017; McClenaghan and Cabri, 2011) in glaciated terrain (McClenaghan, 2005; McClenaghan and Paulen, 2018). More recently, their potential to aid in porphyry copper (Kelley et al., 2011; Hashmi et al., 2015; Plouffe et al., 2016), magmatic Ni–Cu–platinum group elements (PGE; Averill, 2011; McClenaghan and Cabri, 2011), carbonate-hosted Pb-Zn (McClenaghan et al., 2018), and volcanogenic massive-sulfide (VMS) exploration (McClenaghan et al., 2015a, 2017a) has been demonstrated.

Using current sampling protocols, a large till or stream-sediment sample (10–20 kg) is necessary to recover detectable and meaningful numbers of indicator mineral grains for analysis (Plouffe et al., 2013). Indicator minerals are recovered from these large samples at specialized commercial laboratories using a combination of sizing and density concentration methods to reduce the volume of material into a nonferromagnetic heavy-mineral concentrate, referred to in this paper as the HMC, for examination. The resulting HMC is composed of dense mineral grains (specific gravity (SG) >3.2) and the degree of abrasion and wear can be used to infer the transport distance of certain minerals (e.g. DiLabio, 1990; Averill, 2001; McClenaghan et al., 2014a). Mineral associations can be observed in composite grains and the degree of physical liberation of interlocked minerals (e.g. kelyphite rims on Cr-rich garnet in kimberlite dispersal trains) can also indicate the distance of transport (McClenaghan and Kjarsgaard, 2007). The coarse fraction (250–2000 µm; medium to very coarse sand size) of the HMC is visually examined to identify and count indicator minerals using a binocular microscope (McClenaghan, 2011; McClenaghan and Cabri, 2011). Current methods focus on the medium to coarse sand-sized HMC fraction of sediments because it is the most cost effective to recover and visually examine, and the method is well established, having been used for more than 30 years.

Developments in rapid scanning electron microscopy (SEM) such as mineral-liberation analysis (MLA) or quantitative evaluation of minerals by scanning electron microscope (QEMSCAN) during the past 10 years now make it possible to also examine and analyze the fine, less than 250 µm, HMC fraction of sediment samples using automated technologies (Layton-Matthews et al., 2014; Lehtonen et al., 2015). Automated mineralogy provides the potential for the identification and use of additional indicator minerals that traditional visual examination of the 250–2000 µm HMC fraction does not allow. An automated mineralogy method, MLA, was tested using nine archived Geological Survey of Canada (GSC) HMCs of till samples collected near two known polymetallic deposits: the upper-amphibolite–facies Izok Lake VMS deposit (Fig. 1, 2), and the granite-hosted Sisson W-Mo deposit (Fig. 3).

Challenges using fine-grained indicator minerals

Heavy minerals can be concentrated from sediment samples, including till (Averill, 2001; McClenaghan and Paulen, 2018), stream sediments (Wilton and Winter, 2012; McClenaghan et al., 2015b, c; Hulkki et al., 2018), and esker sediments or from disaggregated bedrock (McClenaghan, 2011; Hicken et al., 2013a; McClenaghan et al., 2013a). This study focuses on till, although the methods for handling, sieving, and analyzing the fine-grained HMC fractions described in this paper can be applied to other sample media (e.g. fluvial, alluvial, beach, soils, and bedrock). The size of mineral grains in till reflects the original grain size in bedrock, as well as physical wear and comminution during glacial erosion, transportation, and deposition of the grains. Dreimanis and Vagners (1971) described a bimodal size distribution for specific minerals in till, and the 'terminal' grade at which mineral grains in till become resistant to further comminution. The terminal grade size for most minerals is less than 250 µm; therefore, certain indicator minerals may be more abundant in the less than 250 µm fraction than in the 250 to 2000 µm fraction. The transport distance and grain-size partitioning of this fine, terminal-grade material in till is currently known only for gold grains (Averill, 2001).

Previous analysis by Pickett (2018) of the less than 63 µm HMC fraction of till samples identified cross-contamination during the sample preparation phase as a significant concern. Processing finer grained sample material increases the difficulty in cleaning sieve surfaces because grains are more easily trapped in void spaces, adhere to sieves because of electrostatic forces, or are lost to aerosolization (Lougheed et al., 2019). Trapped grains may not be readily visible, making thorough cleaning of sieves and sieve-cleaning equipment difficult and time consuming. Because low concentrations of indicator minerals (i.e. one or two grains in a 10 kg sample) can constitute a significant 'anomaly', the potential for false-positive results stemming from sample cross-contamination, or false-negative results stemming from lost indicator grains, requires sample handling and sieving measures that mitigate mineral grain loss or cross-contamination (Averill, 2001). To meet this requirement, we used single-use nylon-screened sieves following the methods outlined in Lougheed et al. (2019). Single-use sieves eliminate the potential for sample cross-contamination, grain loss, and the need for time-consuming sieve cleaning.

Mineral-liberation analysis

Mineral-liberation analysis is an automated mineralogy software package used in tandem with a scanning electron microscope (SEM) equipped with energy dispersive spectrometry (EDS) detectors. The software uses high-resolution backscattered electron (BSE) images, image analysis, and elemental chemistry from EDS to create a mosaic image of an epoxy grain mount. The MLA software delineates grain boundaries based on BSE

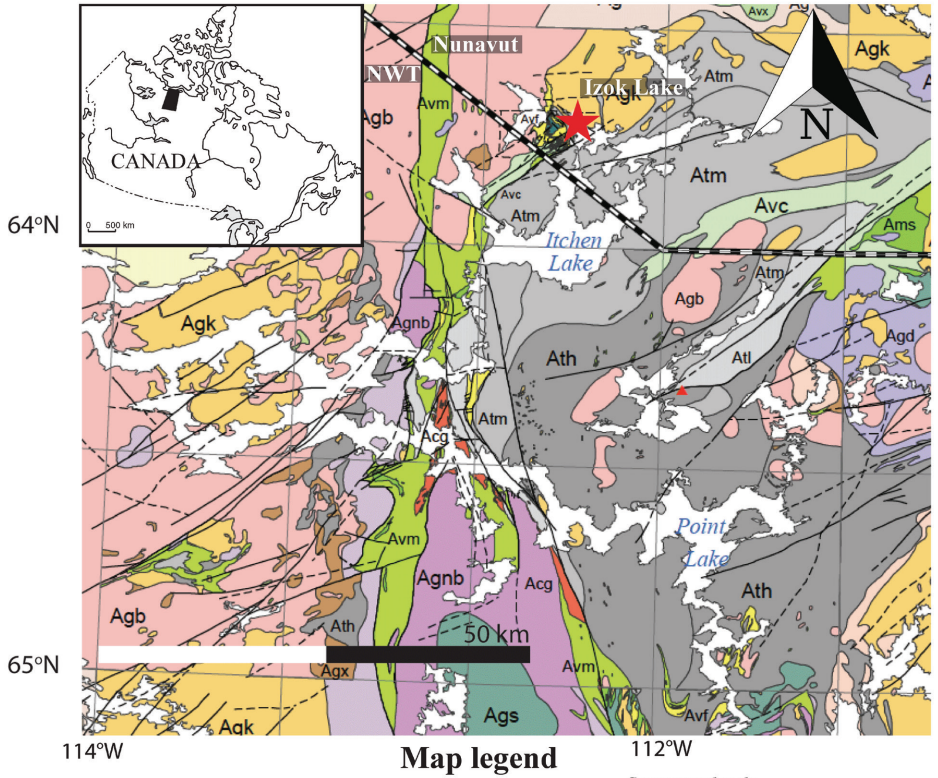

Map legend

Proterozoic

- Pg — Diabase–gabbro sills and/or dykes; various ages
- Pt — Paleoproterozoic foredeep facies; primary greywacke and pelite (turbidites)
- Psc — Paleoproterozoic shelf (± rift) facies dominated by carbonate rocks (dolomite, dololutite, stromatolites)
- Psq — Paleoproterozoic shelf/alluvial (± rift) facies dominated by argillite, quartzite, and conglomerate with lesser carbonate
- Pu — Unsubdivided Proterozoic (± Archean) gabbro, granitoids, sedimentary and volcanic rocks; mixed-age rocks in principal tectonic zones

Archean

Intrusive rocks

- Ag — Granitoids – unsubdivided; includes intrusions with minimal published descriptions or which are not characteristic of other subdivisions
- Agk — Granitoids – 2-mica or K-feldspar megacrystic, pegmatite, mostly syn- to post-kinematic (ca. 2605–2580 Ma)
- Agb — Biotite ± hornblende-rich granitoids, mostly pre- to syn-kinematic (ca. 2625–2590 Ma); includes Agbm unit
- Agbm — Biotite ± hornblende-rich granitoids, mostly pre- to syn-kinematic (ca. 2625–2590 Ma); enhanced magnetic signature
- Agx — Granitoids with abundant supracrustal/gabbro/gneiss xenoliths
- Ams — Mafic intrusions (gabbro, anorthosite, diorite) associated with volcanic rocks; various ages represented but most assumed to be synvolcanic

Supracrustal rocks

Keskarrah formation

- Acg — Conglomerate–arenite–siltstone clastic sequence (mostly <2605 Ma)

Contwoyto formation

- Atm — Turbiditic wacke to mudstone–medium grade; knotted schists (andalusite and/or cordierite porphyroblasts)
- Ath — Turbiditic wacke to mudstone– high grade to migmatitic (sillimanite grade and or anatectic melt phases)

Banting group

- Avm — Volcanic rocks–mafic to intermediate lavas, volcaniclastics, and related intrusions
- Avx — Volcanic rocks–heterogenous interlayered felsic to mafic lavas, volcaniclastics, and related intrusions
- Avc — Volcaniclastic rocks–unsubdivided
- Avf — Volcanic rocks–felsic to intermediate lavas, volcaniclastics, and related intrusions; local carbonate interbeds

Central Slave basement gneissic complexes

- Agnb — Gneiss and granitoid complex–heterogeneous; in part, with demonstrated or assumed 'basement' (>2.8 Ga) components
- Agn — Gneiss and granitoid complex–heterogeneous and unsubdivided; massive to migmatitic and gneissic granitoids; various ages represented

Symbols

- Kimberlites (approximate location)
- Faults; shear zones (defined; probable); NB. numerous reverse faults omitted from Proterozoic orogens
- Location of Izok Lake deposit
- NWT–Nunavut border

Figure 1. Geological map of the Izok Lake region, northwest Slave Province, Nunavut, Canada. The location of the Izok Lake deposit within the belt is indicated by the red star. Heavy black and white dashed line indicates the Northwest Territories (south and west)–Nunavut (north and east) border. Geology from Stubley and Irwin (2019).

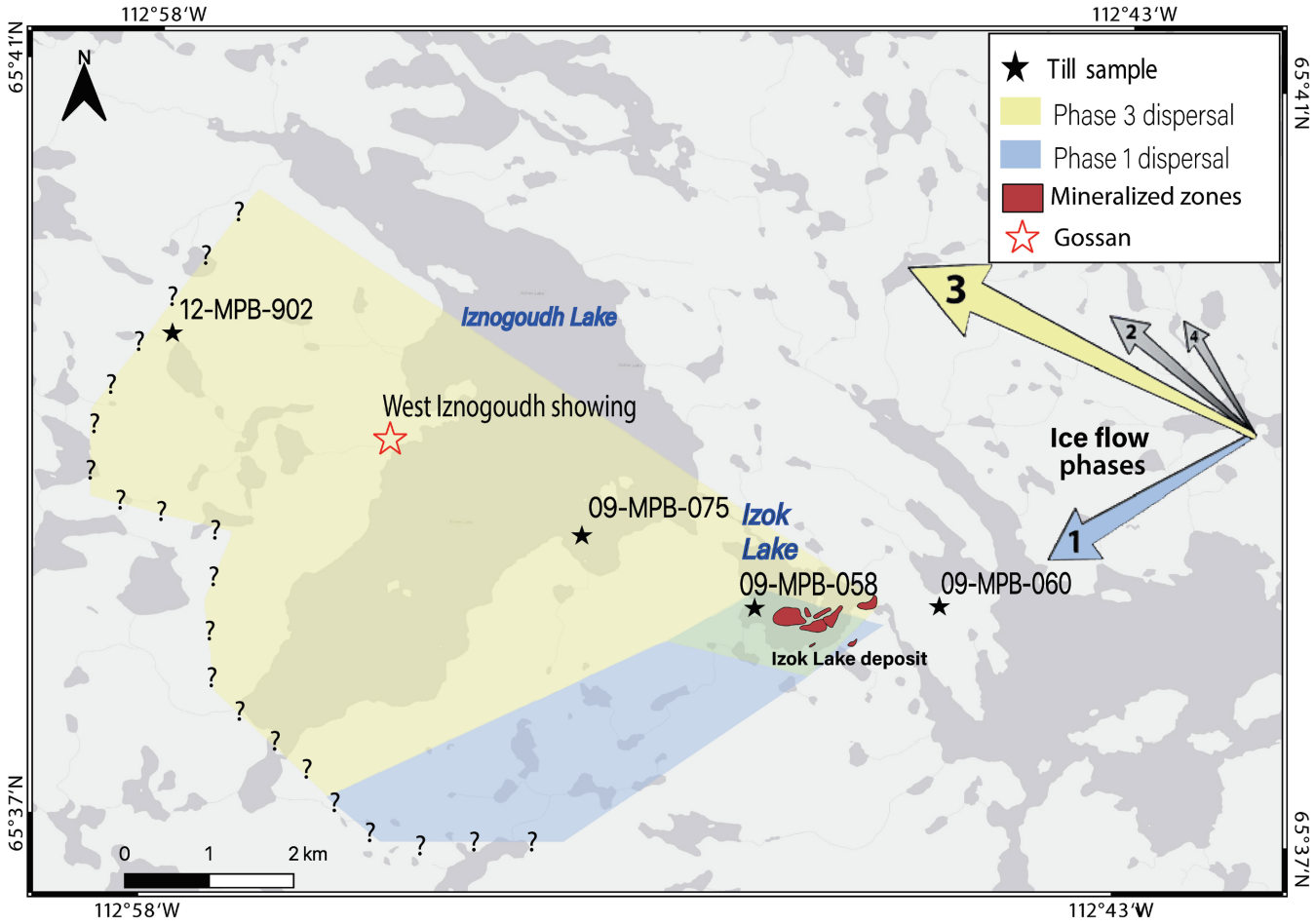

Figure 2. Location of the four studied till samples from the Izok Lake volcanogenic massive-sulfide deposit, Nunavut. Arrows indicate relative chronology (1 = oldest) and vigour (arrow width) of ice-flow events (Paulen et al., 2013). Coloured polygons depict the glacial dispersal fan for gahnite in the nonferromagnetic 250 to 500 µm HMC fraction of till, as interpreted by McClenaghan et al. (2015a). Question marks denote the extent of till sampling, beyond which data are not available.

brightness and contrast and collects a full X-ray spectrum (using EDS) at the geometric centre of each grain, then compares this to an established EDS mineral library assembled by the user to identify the mineral (Sylvester, 2012). Classified grains are subsequently combined into a false-colour mineral image, and the software can quickly calculate size, mineral associations (occurrence and interlocking), particle properties (roundness, area, shape), and mineral liberation for each mineral grain (Layton-Matthews et al., 2014).

The parameters that can be generated and queried by MLA (modal mineralogy, mineral associations, grain size, and grain angularity) would be impractical to manually measure for every grain in a sample. Thus, automated SEM-based techniques can capture data that are indiscernible to the eye (spectral EDS imagery) and morphological data that would be impossible to measure for every grain. These data are collected simultaneously during a single SEM scan and, once collected, can be manipulated by a user to examine individual parameters (e.g. prevalence of a single mineral phase) or the relationships between parameters (e.g. grain-size distributions for individual minerals, mineral- association data).

Because the number of grains available for analysis on a polished mount of a given size increases exponentially with decreasing grain size (Averill and Huneault, 2016), the use of automated mineralogy on less than 250 µm HMC fractions allows for rapid, efficient, and cost-effective collection of large amounts of precise, quantitative data for thousands of mineral grains.

The less than 250 µm fractions of processed HMCs produced in mineral exploration and government till sampling surveys can be pulverized and analyzed geochemically (e.g. Day et al., 2007; Falck et al., 2015). Commonly, the less than 250 µm HMC fraction is archived without analysis immediately after they are produced during sample processing to recover the coarse (250–2000 µm) HMC fraction. Using this archived finer fraction presents an opportunity to gain

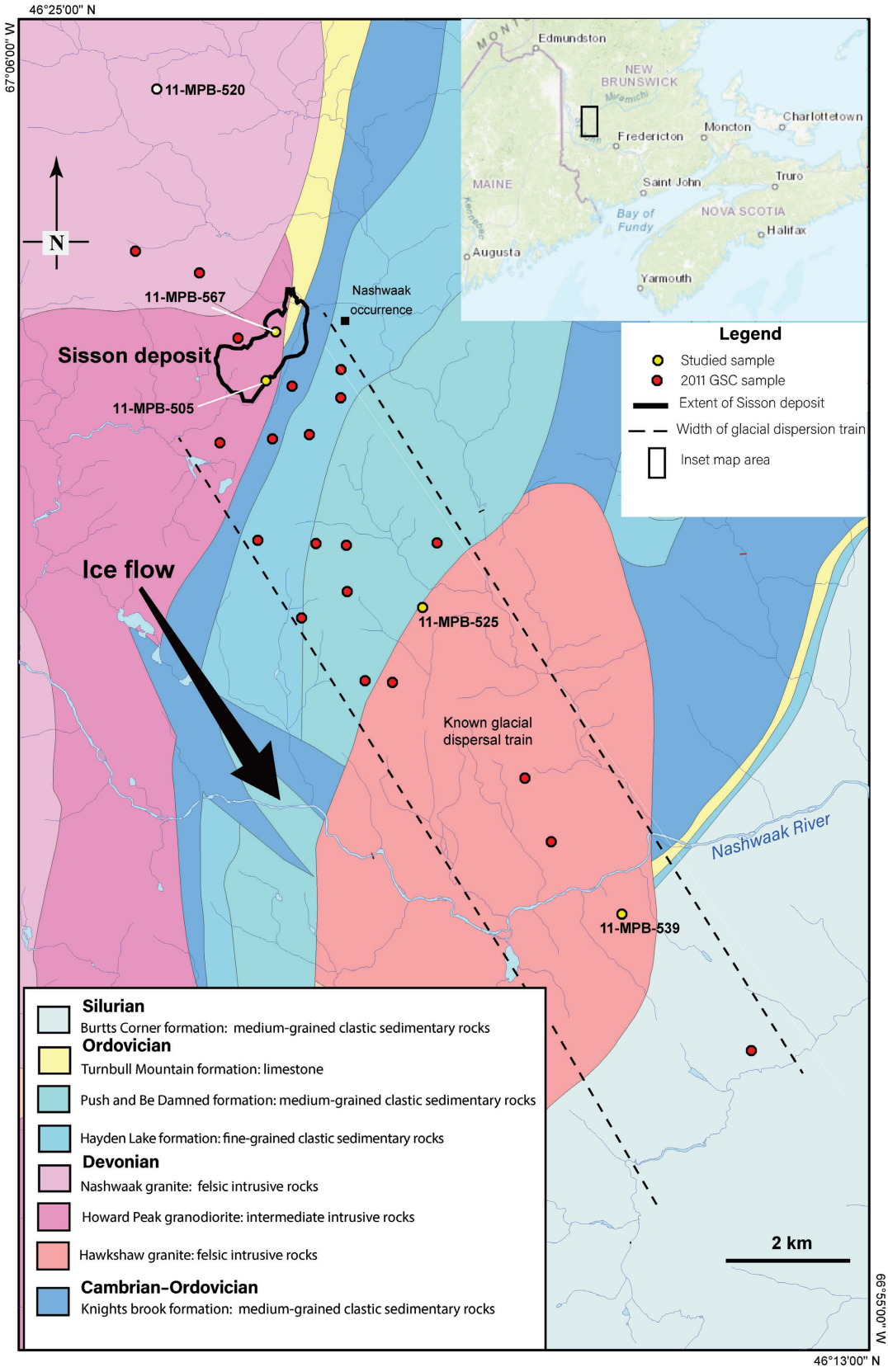

Figure 3. Location of the five studied till samples (yellow dots) from the Sisson granite-hosted W-Mo deposit, New Brunswick. Red dots indicate location of till samples collected by the Geological Survey of Canada in 2011 (McClenaghan et al., 2013a). *Modified* from McClenaghan et al. (2017b).

new geological insights without the added cost of revisiting the sample site or processing additional bulk samples. False-colour mineralogy maps generated by MLA can be used to rapidly identify indicator minerals that are known to be in the coarser HMC fraction of samples, other indicator minerals that were not previously reported (especially those occurring only as inclusions within other minerals), and additional minerals that could assist in characterizing the overall bedrock geological sources of the till. Selected minerals of interest can then be examined further using more sensitive elemental techniques such as laser-ablation inductively coupled plasma mass spectrometry (LA-ICP-MS) or electron probe microanalysis (EPMA).

For this study, the less than 250 µm HMC fractions of nine till samples from two test sites—the Izok Lake Zn-Cu-Pb-Ag VMS deposit in Nunavut and the Sisson W-Mo deposit in New Brunswick—were examined using MLA techniques. These test sites were chosen because till samples have been collected by the GSC at both sites to characterize the heavy-mineral signatures in the 250 to 2000 µm fraction (Hicken et al., 2012, 2013a, b; McClenaghan et al., 2012, 2014b, 2015a). The coarse (250–2000 µm) HMC fraction of each sample was visually sorted to identify and determine indicator mineral abundance. These deposits display well-defined dispersal trains of common indicator minerals extending down ice of each deposit (McClenaghan et al., 2015a) and the indicator abundance data from the 250 to 2000 µm HMC fraction can be compared to data collected using MLA of the less than 250 µm fraction.

Sample suites

Izok Lake

Four till samples collected in 2009 and 2012 by Hicken et al. (2013b) were chosen for this study based on their locations relative to mineralization (Fig. 2) and the indicator minerals present in the 250 to 2000 µm HMC fraction, particularly gahnite. Sample 09-MPB-060 is the sample farthest up-ice (1 km east of mineralization) available for our study and was chosen to represent background values compared to down-ice (west) samples; however, this sample site is still within the hydrothermal alteration halo surrounding the Izok Lake deposit (Morrison, 2004), and may not represent true regional background for alteration minerals. Sample 09-MPB-058, located 500 m down ice (west) of mineralization, is the only sample from this study that contains a significant number of sulfide indicator minerals in the coarse fraction (Hicken et al., 2013b) and is the most proximal down-ice sample chosen for this study. Sample 09-MPB-075, located 3 km down ice of mineralization, is an intermediate down-ice sample and sample 12-MPB-902, located 8 km down ice of mineralization, is the most distal down-ice sample examined in this study.

Sisson

Five till samples collected in 2011 by McClenaghan et al. (2013a; 2014b; 2015b, c) were chosen for this study based on their locations relative to mineralization (Fig. 3) and the indicator mineral content in the 250 to 2000 µm HMC fraction. Sample 11-MPB-520 is the farthest up-ice till sample available (4 km from mineralization) and was chosen to represent background values compared to down-ice sample locations. Samples 11-MPB-505 and 11-MPB-567 overlie the mineralization: sample 11-MPB-505 overlies the Ellipse zone and sample 11-MPB-567 overlies zone III. Samples 11-MPB-525 and 11-MPB-539 (4.3 and 10 km down ice of mineralization, respectively) represent proximal and distal down-ice samples, respectively, within the known dispersal train. Previous work identified the ore mineral scheelite in the coarse (250–2000 µm) HMC fraction of till from each of the four overlying and down-ice sites (McClenaghan et al. 2013a; 2014b; 2015b, c).

Geological setting of test sites

Izok Lake

Bedrock and deposit geology

The Izok Lake VMS deposit is located in the central Slave Province, a granitic greenstone terrane comprising deformed and metamorphosed Archean rocks hosting the Yellowknife Supergroup, a package of 2.70 to 2.67 Ga metasedimentary and metavolcanic rocks (Bleeker and Hall, 2007). The Yellowknife Supergroup is divided into the lower Point Lake Formation (a suite of mafic tholeiitic to felsic calc-alkaline metavolcanic rocks and derived metasedimentary rocks) and the upper Contwoyto Formation (a series of iron formation–bearing greywacke turbidites; Fig. 1). These formations host numerous granitic plutons along with north-northwest–trending regional diabase dykes of the Helikian Mackenzie Swarm (Bleeker et al., 1999; Buchan and Ernst, 2004).

Rocks south of the deposit have been metamorphosed under greenschist-facies conditions and have a mineral assemblage of albite-epidote-chlorite, whereas rocks to the north are upper-amphibolite to sillimanite grade with a mineral assemblage of calcic amphibole–cordierite–sillimanite (Thomas, 1978). The variance in metamorphic grade was interpreted by Thomas (1978) to be the result of two regional metamorphic events but this idea was challenged first by Morrison (2004) and later by Nowak (2012). They suggested that the rocks in the region were affected by a single, craton-wide, high-temperature, low-pressure event. This conclusion is supported by similarities between pressure and temperature estimates from mineral assemblages at Izok Lake and other rocks from the Slave Craton (Morrison, 2004), whereas the local variation in metamorphic mineral assemblages identified is attributed to variations in pre-metamorphic bulk rock composition brought about by varying degrees of hydrothermal alteration (Nowak, 2012).

Mineralized boulders containing greater than 30 weight per cent Zn were discovered along the west and south shores of Izok Lake by Money and Heslop (1976); this initiated more detailed local exploration and the discovery of the Izok Lake deposit. The deposit consists mainly of sphalerite, chalcopyrite, and galena, with a variety of other less abundant ore minerals including covellite, digenite, electrum, and native silver (Money and Heslop, 1976; Morrison and Balint, 1993; Morrison, 2004). Izok Lake is a significant base-metal resource, with total indicated and inferred resources of 14 800 000 t grading 12.8 weight per cent Zn, 2.5 weight per cent Cu, 1.3 weight per cent Pb, and 71 g/t Ag contained in five sulfide lenses (North, Northwest, Central West, Central East, and Inukshuk; Costello et al., 2012), making it one of the largest undeveloped Zn-Cu resources in North America (Morrison, 2004). The three westernmost lenses (North, Northwest, and Central West) subcrop under Izok Lake and thus were exposed to glaciation, whereas the two easternmost lenses (Central East and Inukshuk) are stratigraphically deeper and have not been exposed to glaciation.

The minerals present in the Izok Lake deposit and its alteration zones that might be found in till samples examined in this study are summarized in Table 1, based on McClenaghan et al. (2015a). Rocks in the footwall of the deposit and to the north have been interpreted as a rhyolite precursor metamorphosed to upper amphibolite to sillimanite grade with characteristic mineral assemblages of calcic amphibole, cordierite, and sillimanite. Hanging-wall rocks are interpreted as meta-andesite (cordierite-biotite-epidote-garnet), aphyric meta-rhyolite (quartz-muscovite-sillimanite-garnet), and metagabbro (amphibole-plagioclase-biotite-garnet-magnetite). Gahnite (Zn spinel) is a metamorphic mineral in stringer-sulfide mineralized zones proximal to the deposit's five sulfide lenses. It was identified by Hicken et al. (2013a, b) and McClenaghan et al. (2015a) as a useful indicator of mineralization at Izok Lake and is present in a glacial dispersal fan up to 40 km down ice of the deposit. In the deposit, gahnite is intergrown with quartz, feldspar, biotite, muscovite, sphalerite, chalcopyrite, and pyrrhotite (Morrison, 2004; Nowak, 2012; Hicken et al., 2013a).

Surficial geology

The Izok Lake region was most recently glaciated during the Wisconsinian (Dredge et al., 1996a). Regional surficial mapping in the Izok Lake region was carried out by Dredge et al. (1999) and Stea et al. (2009), with large-scale ice-flow reconstructions compiled by Dyke and Prest (1987a, b) and Dyke (2004). Recent ice-flow indicator mapping in the region by Paulen et al. (2013) built on the previous work and elucidated four ice-flow phases that affected the region. Of these, an older, southwest ice flow and younger northwest ice flow were determined to be responsible for the formation of most local glacial landforms and the palimpsest glacial transport of mineralized debris down ice (Hicken et al., 2013b; McClenaghan et al., 2015a). These ice flows deposited a thin (<3 m thick) till layer with an unsorted matrix of silty sand (Hicken et al., 2013b), ideal for testing methods for identifying indicator minerals of a wide range of grain sizes. The Izok Lake region is a permafrost-covered terrain; therefore, all samples were collected at surface from frost boils—small, circular, periglacial features formed by cryoturbation that bring fresh till from depth to surface (Shilts, 1978).

Previous surficial geochemical and indicator mineral studies

The GSC carried out a reconnaissance-scale till geochemical survey in the Point Lake region, including the Izok Lake area in 1994, but till matrix geochemical analysis of the widely spaced regional till samples did not indicate the presence of the mineralization at Izok Lake (Dredge et al., 1996b). In 2009, higher density till sampling for indicator mineral and till geochemistry analysis was carried out around the Izok Lake deposit and the nearby West Iznogoudh (WIZ) showing (Oviatt, 2010; Hicken, 2012). The less than 63 µm fraction of till, analyzed by aqua regia followed by ICP-MS, yielded high concentrations of Cu, Pb, Zn, and other associated metals up to 6 km down ice (to the northwest; McClenaghan et al., 2015a). One goal of our study was to ascertain whether the till geochemical signatures associated with the Izok Lake deposit are reflected in the mineralogy of the less than 250 µm HMC fraction of till.

The primary focus of the 2009 study was the mineralogy of the 250 to 2000 µm HMC fraction. The GSC identified gahnite, staurolite, chalcopyrite, sphalerite, pyrrhotite, and pyrite as indicator minerals in till overlying and down ice of the deposit (Hicken, 2012; McClenaghan et al., 2015a). Gahnite dispersal was the broadest and farthest down ice of all of the indicator minerals, extending more than 40 km to the northwest (Hicken et al., 2013b; McClenaghan et al., 2015a). Abundant sulfide minerals (chalcopyrite, galena, sphalerite, and pyrite) were identified in the coarse fraction of only the most proximal (500 m) down-ice till sample (09-MPB-058).

Sisson

Bedrock and deposit geology

The sub-greenschist Sisson deposit is a granite-hosted, W-Mo deposit located in west-central New Brunswick (Fig. 3), on the eastern margin of a belt of plutonic rocks emplaced during the Acadian Orogeny (Late Silurian to Early Devonian) and underlying the Miramichi Highlands (Fyffe et al., 2008). The deposit is closely associated with felsic magmas emplaced into clastic sedimentary rocks of the Cambrian to Early Ordovician Miramichi Group, the volcanic and sedimentary rocks of the Ordovician Tetagouche Group, and deformed Ordovician plutonic

Table 1. Summary of metallic minerals in the Izok Lake volcanogenic massive-sulfide (VMS) deposit, Nunavut.

Mineral	Formula	Hardness	Specific gravity	Presence in bedrock or till reported by other sources
Metallic minerals				
Acanthite	Ag_2S	2.0–2.5	7.2–7.4	Harris et al. (1984b)
Allargentum	$Ag^{1-x}Sb^x(x\text{-}0.009–0.16)$	4.0	10.0	Harris et al. (1984b)
Arsenopyrite	FeAsS	5.0	6.1	Harris et al. (1984b)
Boulangerite	$Pb_5Sb_4S_{11}$	2.5	5.7–6.3	Harris et al. (1984b)
Bournonite	$PbCuSbS_3$	3.0	5.7–5.9	Harris et al. (1984b)
Breithauptite	NiSb	3.5–4.0	8.2	Harris et al. (1984b)
Chalcopyrite	$CuFeS_2$	3.5	4.1–4.3	Money and Heslop (1976), Cabri et al. (1984) and Harris et al. (1984b)
Cobaltite	CoAsS	5.5	6.3	Harris et al. (1984b)
Cosalite	$Pb_2Bi_2S_5$	2.5–3.0	6.4–6.8	Harris et al. (1984b)
Covellite	CuS	1.5–2.0	4.6–4.8	Harris et al. (1984b)
Cubanite	$CuFe_2S_3$	3.5	4.7	Harris et al. (1984b)
Digenite	Cu_9S_5	2.5–3.0	5.6	Harris et al. (1984b)
Dyscrasite	Ag_3Sb	3.5–4.0	9.4–10.0	Harris et al. (1984b)
Electrum	AuAg	2.5–3.0	16.0	Harris et al. (1984b)
Galena	PbS	2.5	7.2–7.6	Money and Heslop (1976) and Harris et al. (1984b)
Gudmandite	FeSbS	5.5–6.0	6.7	Harris et al. (1984b)
Izoklakeite	$(Cu, Fe)_2Pb_{27}(Sb, Bi)_{19}S_{57}$	3.5–4.0	6.5	Harris et al. (1986)
Jaskolskiite	$Cu_{0.2}Pb_{2.2}Sb_{1.2}Bi_{0.8}S_5$	4.0	6.5	Harris et al. (1984a)
Loellingite	$FeAs_2$	7.1–7.5	5.0–5.5	McClenaghan et al. (2015a)
Meneghinite	$Pb_{13}CuSb_7S_{24}$	2.5	6.3–6.4	Harris et al. (1984b)
Molydenite	MoS_2	1.0	5.5	Harris et al. (1984b)
Native bismuth	Bi	2.0–2.5	9.7–9.8	Harris et al. (1984b)
Native silver	Ag	2.5–3.0	10.0–11.0	Harris et al. (1984b)
Nuffieldite	$Pb_2Cu(Pb, Bi)Bi_2S_7$	3.5–4.0	7.0	Harris et al. (1984b)
Polybasite	$[(Ag,Cu)_6(Sb,As)_2S_7][Ag_9CuS_4]$	2.5–3.0	4.6–5.0	Money and Heslop (1976) and Harris et al. (1984b)
Pyrargyrite	Ag_3SbS_3	2.5	5.9	Harris et al. (1984b)
Pyrite	FeS_2	6.5	5.0–5.2	Money and Heslop (1976), Harris et al. (1984b), and Morrison and Balint (1993)

Data reported by Money and Heslop (1976), Cabri et al. (1984), Harris et al. (1984a, b, 1986), and Morrison and Balint (1993; *modified from* McClenaghan et al. (2015a)) and oxide and silicate indicator minerals of base-metal VMS deposits in glaciated terrain was reported by McClenaghan et al (2015a).

Table 1. (cont.) Summary of metallic minerals in the Izok Lake volcanogenic massive-sulfide (VMS) deposit, Nunavut.

Mineral	Formula	Hardness	Specific gravity	Presence in bedrock or till reported by other sources
Sphalerite	(Zn,Fe)S	3.5–4.0	3.9–4.2	Money and Heslop (1976), Harris et al. (1984b), and Morrison and Balint (1993)
Stannite	Cu_2FeSnS_4	3.5–4.0	4.3–4.5	Harris et al. (1984b)
Stephanite	Ag_5SbS_4	2.0–2.5	6.2–6.3	Harris et al. (1984b)
Sternbergite	$AgFe_2S_3$	1.0–1.5	4.2	Harris et al. (1984b)
Tennantite	$(Cu,Fe)_{12}As_4S_{13}$	3.5–4.0	4.6–4.7	Harris et al. (1984b)
Tetrahedrite	$(Cu,Fe)_{12}Sb_4S_{13}$	3.5–4.0	4.6–5.2	Money and Heslop (1976) and Harris et al. (1984b)
Valleriite	$4(Fe,Cu)S•3(Mg,Al)(OH)_2$	1.0–1.5	3.1	Harris et al. (1984b)
Oxide and silicate indicator minerals				
Anthophyllite§	$(Mg,Fe)_7Si_8O_{22}(OH)_2$	5.0–6.0	3.5	No
Barite§	$BaSO_4$	4.5	3.0–3.5	No
Cassiterite	SnO_2	6.0–7.0	6.8–7.0	Harris et al. (1984b)
Cr-Rutile§	$(Ti,Cr)O_2$	6.0–6.5	4.2	McClenaghan et al. (2015a)
Dumortierite§	$Al_7(BO_3)(SiO_4)_3O_3$	7.0–8.5	3.3–3.4	No
Franklinite§	$(Zn,Mn,Fe)(Fe,Mn)_2O_4$	5.5–6.0	5.0–5.2	No
Gahnite§	$ZnAl_2O_4$	8.0	4.0–4.6	Money and Heslop (1976) and Morrison and Balint (1993)
Kyanite§	Al_2SiO_5	4.0–7.0	3.6	McClenaghan et al. (2015a)
Mg-Spinel§	$MgAl_2O_4$	8.0	3.6	No
Mn-Epidote§	$Ca_2(Al,Fe,Mn)_3Si_3O_{12}(OH)$	6.0–7.0	3.3–3.6	McClenaghan et al. (2015a)
Orthopyroxene§	$(Mg,Fe)_2Si_2O_6$	5.0–6.0	3.4	McClenaghan et al. (2015a)
Sapphirine§	$(Mg,Al)_8(Al,Si)_6O_{20}$	7.5	3.5	No
Sillimanite§	Al_2SiO_5	6.5–7.5	3.2	Morrison and Balint (1993)
Spessartine§	$Mn_3Al_2Si_3O_{12}$	6.5–7.5	4.2	Morrison and Balint (1993)
Staurolite§	$(Fe,Mg,Zn)_2Al_9(Si,Al)_4O_{22}(OH)_2$	7.0–7.5	3.7–3.8	McClenaghan et al. (2015a)
Tourmaline§	$(Na,Ca)(Mg,Fe)_3Al_6(BO_3)_3(Si_6O_{18})(OH)_4$	7.0–7.5	3.1	McClenaghan et al. (2015a)
Willemite§	$ZnSiO_4$	5.5	3.9–4.2	No
Magnetite	Fe_3O_4	5.5–6.0	5.1–5.2	Morrison and Balint (1993)
Mn-Axinite	$Ca_2MnAl_2(BO_3)Si_4O_{12}(OH)$	6.5–7.0	3.3	McClenaghan et al. (2015a)

§Averill (2001)
Data reported by Money and Heslop (1976), Cabri et al. (1984), Harris et al. (1984a, b, 1986), and Morrison and Balint (1993; *modified from* McClenaghan et al. (2015a)) and oxide and silicate indicator minerals of base-metal VMS deposits in glaciated terrain was reported by McClenaghan et al (2015a).

rocks (van Staal, 1991). Two plutons are spatially related to the Sisson deposit: the Howard Peak granodiorite and the Nashwaak granite (Fyffe et al., 1981). The regional host rocks were later intruded by a phaneritic felsic dyke swarm and a distinctively younger Late Devonian porphyritic felsic dyke (Zhang et al., 2013). Mineralization at Sisson is hosted within the eastern margin of the Howard Peak granodiorite, where it is in contact with Cambrian to Early Ordovician volcanic and sedimentary rocks.

The Sisson deposit is hosted in three mineralized zones. Zones I and II are structurally controlled, are wide (>10 m) and approximately 100 m along strike (Zhang et al., 2016). Zone I is hosted within a thin-bedded sequence of dark grey siltstone and tuff and zone II is hosted in gabbroic rocks; both are associated with quartz veins in a highly silicified shear zone. Zone III, the main ore resource for the deposit, is hosted by sheared and silicified gabbroic rocks of the Howard Peak pluton, with associated cataclastically deformed granitic dykes that likely represent apophyses of the Nashwaak pluton (Fyffe et al., 2008; Zhang et al., 2016). Mineralization in zones I and II primarily consists of wolframite and chalcopyrite, concentrated primarily in late stockworks, whereas zone III is composed of scheelite and molybdenite, which occur in early and late veins and stockworks (Nast and Williams-Jones, 1991; Fyffe et al., 2008). Hydrothermal alteration is concentrated in the immediate vicinity of veins and fractures, and pervasive throughout a large area surrounding the deposit. Rennie et al (2013) reported resource estimates for the deposit of 383 000 000 t at 0.069 weight per cent WO_3 and 0.023 weight per cent Mo (proven) and an additional 178 000 000 t at 0.065 weight per cent WO_3 and 0.020 weight per cent Mo (probable).

Surficial geology

Mineralization subcrops beneath the local till cover. Bedrock outcrops in the area are rare due to a continuous till cover that varies from less than 2 to 20 m in thickness. Most of this thick till cover is a sandy lodgment till deposited by southeast glacial flow during the early Wisconsinan. This till may have been reworked by subsequent south-southwest glacial flow during the middle to late Wisconsinan (Seaman and McCoy, 2008). A discontinuous, thin (<2 m), sandy ablation till overlies the early Wisconsinan till in places (Seaman and McCoy, 2008; Fyffe et al., 2010; Stea et al., 2011), but this was avoided during till sampling studies.

Previous surficial geochemical and indicator mineral studies

Reconnaissance-scale surface till geochemical surveys carried out in the region identified a 30 km long glacial dispersal train extending southeast of the Sisson deposit. The train was defined by the various combinations of W, Mo, As, Bi, Cu, F, Pb, and Sn contents in several different size fractions of till (Snow and Coker, 1987; Lamothe, 1992; Seaman, 2003; Seaman et al., 2008 McClenaghan et al., 2013b). Till indicator mineral studies carried out by McClenaghan et al. (2013a, c, 2014b, 2015b, c) combined with stream-sediment indicator mineral data (McClenaghan et al., 2017b) indicate that the 250 to 2000 µm HMC fraction of sediments includes the ore minerals scheelite, wolframite, and molybdenite, and sulfide- and Bi-bearing minerals. Scheelite was found in till samples collected at least 10 km down ice of mineralization, whereas the other ore minerals were only found in till samples immediately overlying mineralization. Scheelite and wolframite were recovered from the 250 to 2000 µm HMC fraction of stream sediments collected at least 4 km downstream of the north end of the deposit, and 5 km to the southeast, downstream from the southeast-trending glacial dispersal train.

METHODS

Heavy-mineral concentrate (HMC) processing

Izok Lake and Sisson till samples were processed at Overburden Drilling Management Ltd. (ODM), Ottawa, Ontario, at the time of the initial GSC heavy-mineral studies to recover greater than 3.2 SG HMCs. Density concentration of samples was carried out using a combination of wet screening and shaking table, followed by heavy-liquid separation at 3.2 SG, acid-washing, and ferromagnetic separation to produce a coarse (250–2000 µm), nonferromagnetic HMC (>3.2 SG) fraction. This coarse fraction was visually examined and indicator minerals were counted, with results reported for Izok Lake by Hicken et al. (2013a, b) and for Sisson by McClenaghan et al. (2015b, c). The archived by-product of sample processing was the nonferromagnetic, less than 250 µm HMC fraction that is the basis of our study. The mass of each fraction produced during sample processing at the Queen's Facility for Isotope Research (QFIR) and analyzed in this study, is presented in Table 2.

Sieving

The less than 250 µm HMC fraction of each sample was too large to be mounted in its entirety, and the range of grain sizes within the samples is too great for the grains to be uniformly exposed in a polished section; therefore, the less than 250 µm HMC fraction was dry sieved into four smaller size fractions—185 to 250 µm, 125 to 185 µm, 64 to 125 µm, and less than 64 µm—at the QFIR. The 64 to 125 µm fraction consists of very fine sand and the less than 64 µm fraction consists of silt- to clay-sized grains. The two coarsest fractions (125–185 µm and 185–250 µm) together represent the fine-sand size fraction. The samples were sieved using single-use, nylon-screened sieves following the procedures developed by Lougheed et al. (2018, 2019).

Table 2. Sample and subsample masses, and mass lost during sieving, for the less than 250 µm heavy-mineral concentrate (HMC) fraction of four till samples from the Izok Lake deposit, Nunavut.

Sample number	Mass of <250 µm fraction (g)	Size fraction (µm)	Mass of fraction (g)	Total mass of four size fractions (g)	Calculated mass lost (g)
09-MPB-060	16.637	185–250	2.668	16.544	0.093
		125–185	5.145		
		64–125	6.624		
		<64	2.107		
09-MPB-058	29.223	185–250	3.426	29.124	0.099
		125–185	7.060		
		64–125	12.064		
		<64	6.574		
09-MPB-075	22.933	185–250	3.132	22.848	0.085
		125–185	5.959		
		64–125	9.584		
		<64	4.173		
12-MPB-902	22.769	185–250	2.949	22.679	0.090
		125–185	4.814		
		64–125	9.716		
		<64	5.200		

Table 2 lists the mass of each less than 250 µm, nonferromagnetic HMC fraction prior to our study, the mass of each size fraction resulting from dry sieving, and the mass lost as a result of sieving for the four Izok Lake samples selected for our study. Sieving of four Izok Lake samples resulted in 16 subsamples, and the five Sisson samples produced 20 subsamples.

Epoxy mounting of mineral grains

The grain-mounting methods we used are based on those used by Lougheed et al. (2020), who modified the methods of Blaskovich (2013). Blaskovich (2013) mixed the entire size fraction of each sample with epoxy resin and allowed it to cure within a cylindrical mould. Following the method described in detail in Lougheed et al. (2020), we mixed the entirety of each subsample with vacuum-evacuated epoxy, poured it into a 25 mm plastic ring mould, and allowed it to cure. Each primary mount was then vertically quartered and one quarter was archived for future reference. The other three quarters were remounted together in a secondary plastic ring mould—one quarter with its base face down and the other two, diagonally opposite quarters from the primary mount, with one cut vertical facet face down (Fig. 4)—set with epoxy, and cured for 12 h. Thus, a secondary epoxy mount containing one basal and two vertical sections was prepared for each subsample. This method was used to prepare all 16 subsamples from the Izok Lake deposit and 5 of 20 subsamples (the 185–250 µm HMC fractions) from the Sisson deposit.

After MLA of vertical and basal slabs of their quartered epoxy mounts, Lougheed et al. (2020) concluded that mounting a consistent mass of sample as a near-monolayer grain mount and using this basal surface for MLA is the optimal mounting method to determine the mineralogy of till HMCs. The 'consistent mass' method described in Lougheed et al. (2020) was used to prepare 15 of the 20 subsamples (the <65, 65–125, and 125–185 µm fractions) of the Sisson deposit samples. Analysis of the five 185 to 250 µm Sisson subsamples was limited to the basally mounted one quarter. These samples allowed comparison between the detection of indicator minerals using the entire basal surface of a mount (506.71 mm^2) versus only one quarter (126.68 mm^2) of that area.

Mineral-liberation analysis methods

All sample mounts examined in this study were carbon-coated prior to MLA analysis. Grain mounts were analyzed in a Field Electron and Ion Company (FEI) Thermo Scientific™ Quanta™ 650 field-emission gun environmental scanning electron microscope equipped with dual EDS detectors operating under high vacuum at QFIR. Operating conditions included a beam current of 10 nA, an accelerating voltage of 25 kV, and a spot size of 6. Backscattered

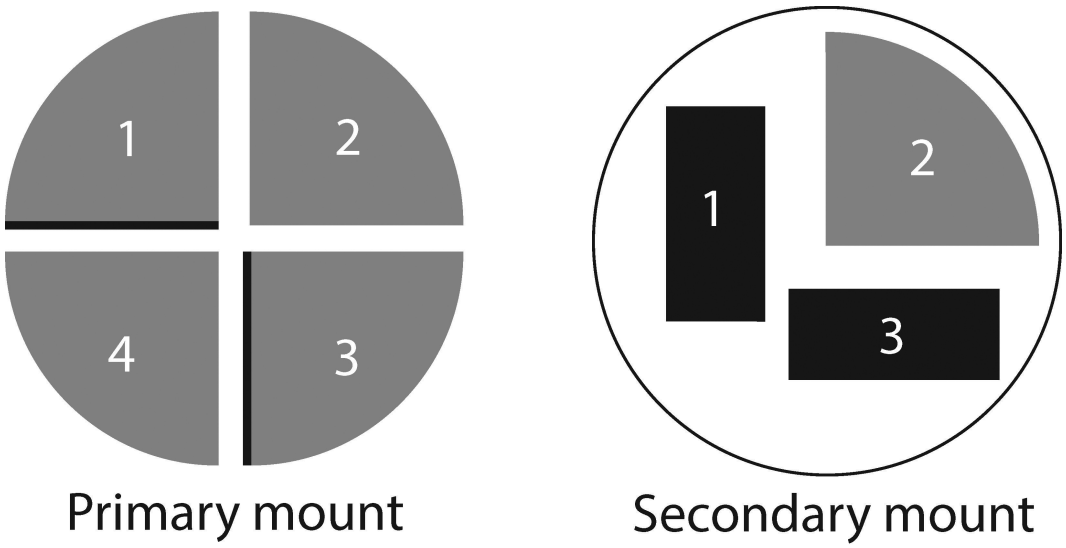

Figure 4. Plan view of the two stages of the epoxy grain mounting method used for all Izok Lake subsamples and the five 185 to 250 µm samples. The primary grain mount was quartered, and three quarters were reoriented on a secondary mount displaying one basal surface (grey) and two cross-sectional surfaces (black) for analysis. The remaining quarter of the primary mount was archived.

electron image brightness and contrast were standardized to an Au imaging standard. Magnification was set to 250× and each basal quarter contained between 75 and 210 frames for analysis, whereas each vertical section contained between 100 and 200 frames. Analysis of the one-quarter, basal surface slab (slab 2 in Fig. 4) of each Izok Lake grain mount took between 35 min and 2.5 h, with the mounts of the less than 64 µm fraction requiring the most time because they contained the most grains. The basal quarter sections of the Izok Lake mounts (slab 2 in Fig. 4) contained between 5000 and 50 000 grains; this range reflects the exponential increase in the number of grains that can be mounted with decreasing grain size (Averill and Huneault, 2016). Scans of Sisson sample basal (whole) sections took between 3 and 4 h per sample, with each mount containing between 20 000 and 300 000 grains. Postprocessing data analysis was performed using MLA Image Processing and Dataview software, product version 3.1.4.686. Areas obscured by charging effects were removed from the false-colour maps and each remaining grain was classified using a mineral reference library constructed from spectra from the FEI reference library and gathered over several years at QFIR.

Reporting

Several reporting metrics can be generated by automated mineralogical software packages, including weight per cent, volume per cent, grain count, and proportion covered (area per cent). Simandl et al. (2015) noted a high coefficient of determination ($R^2 = 0.90$) between the weight per cent estimates of Nb-bearing minerals (fersmite, pyrochlore, and columbite) in stream sediments using QEMSCAN® and total Nb content determined by X-ray fluorescence spectrometry, and a similarly high R^2 value for monazite abundance plotted against rare-earth element (REE; ΣLa, Ce, Pr, Nd) content determined by borate fusion–nitric acid digestion followed by ICP-MS; however, these REEs are not commonly present in a wide range of minerals. Methods of determining weight per cent within automated mineralogy software packages either assume perfect mineral stoichiometry or require mineral chemistry data (i.e. EPMA); therefore, weight per cent values are not appropriate for reporting the abundance of most minerals that have varying stoichiometry, or where the elements of interest commonly occur in multiple mineral phases.

The calculation of 3-D volume per cent from a 2-D surface requires the generalization of a grain's volume as a sphere or ellipse using the length of the long axis present on the polished grain surface (Sylvester, 2012). This is a powerful tool for many applications of automated mineralogy because it allows the user to establish a 'grade' for a sample by combining mineral chemistry data with the resultant volume from MLA, but it is unnecessary for indicator mineral exploration when the only target is the relative abundance of an indicator mineral, and the interpretation of data is not enhanced by extrapolating 2-D data into 3-D data.

Although grain counts are an intuitive metric for understanding indicator-mineral abundance and are more easily related to traditional visual grain counts of the 250 to 2000 µm HMC fraction, a small amount of uncertainty is introduced by the MLA software when it defines and separates grain boundaries. Grains are defined as the homogeneous fraction of a mineral and can be an entire monomineralic particle, or part of a composite particle composed of grains of several

minerals. Proportion covered (area per cent) is calculated by dividing the number of pixels assigned to a specific mineral value by the total number of pixels measured. This calculation provides a metric that, although less intuitive than grain counts, represents a more precise quantitative measure.

Proportion covered (area per cent) can be used in tandem with the number of grains to discern information about the occurrence of indicator minerals that would not be observed using either metric alone. Low grain counts corresponding with a high relative proportion covered suggest that a mineral is present as discrete whole grains (Fig. 5). High grain counts combined with a low proportion covered suggest that a mineral is present as a large number of smaller grains or disseminated inclusions in other mineral grains. These conclusions must be confirmed by observing the mineral in a false-colour MLA grain map. When using grain counts, it is important to normalize values to allow for comparison between samples containing varying numbers of grains. Hulkki et al. (2018) used two methods for normalizing grain count data. Their disaggregated bedrock samples were normalized to indicator grains per 1000 total grains using the equation:

(Number of grains of a specific indicator mineral in a sample

/Total number of mineral grains in sample) × 1000

This ratio accounts for the variation in the total number of grains between samples. In contrast, Hulkki et al. (2018) normalized stream-sediment grain counts to a 1 kg processed sample weight, although the authors noted that, given the extremely low abundance of the copper minerals of interest, the normalized values were very close to the numbers of observed mineral grains.

Normalizing to the total processed sample weight does not take into account the varying number of grains analyzed among the different size fractions studied, which can range between tens of thousands of grains on a 185 to 250 µm sample mount and hundreds of thousands on a less than 64 µm sample mount. Normalizing to indicator grains per 1000 grains allows for comparison of abundance values between samples, and between different size fractions of the same sample. Values in this study were normalized to indicator grains per 1000 grains using the bedrock sample method used by Hulkki et al. (2018).

The abundance of each indicator mineral in each sample surface in this study is reported in Tables 3 to 8 as the number of indicator grains normalized to grains per 1000 total grains and as the proportion of the sample covered by the mineral (area per cent).

RESULTS

Izok Lake

The four size fractions of all four Izok Lake till samples are dominated by calcic amphibole, ilmenite, and almandine. Minerals present in lesser abundance include epidote, chlorite, biotite, titanite, rutile, and assorted Fe-oxide minerals (Fig. 6). Quartz and albite, both less dense than the 3.2 SG heavy liquid used to process the original till samples, occur in high abundance in all samples, primarily as parts of composite grains containing other denser minerals. Abundances increase with decreasing grain size for ilmenite, almandine, epidote, rutile, titanite, apatite, zircon, and monazite. Quartz, chlorite, and biotite decrease in abundance with decreasing grain size.

Secondary minerals (e.g. goethite, jarosite) in till have previously been identified as indicator minerals by McClenaghan et al. (2017a). These minerals can be derived from preglacial gossans entrained by glacial processes, or from in situ postglacial weathering of sulfide grains in till. Iron oxide minerals were identified in all size fractions of all samples from Izok Lake, with a notable increase in abundance in the 185 to 250 µm fraction in the samples collected down ice of mineralization (Fig. 6).Epidote is present in the highest relative abundance in the 64 to 125 and less than 64 µm fractions of samples 09-MPB-060, 09-MPB-058, and 090-MPB-075, as well as the 125 to 185 µm fraction of sample 09-MPB-058 (Fig. 6; Table 4).

The ore minerals present in samples are chalcopyrite, sphalerite, pyrite, and galena (Table 3). Sulfide minerals are present in the highest abundance in sample 09-MPB-058, the most proximal down-ice sample to sulfide mineralization. Established indicator minerals of high metamorphic grade VMS deposits (Averill, 2001) identified in the samples include gahnite (Zn spinel), corundum, staurolite, epidote, and Fe-oxide (Table 4).

Alteration minerals and metamorphic equivalents

Gahnite is present in all four samples with values ranging from 0.031 to 4.529 normalized grains per 1000 grains. Sample 09-MPB-058, contains the most gahnite (0.900–4.529) of the four samples. Gahnite is three times more abundant in the 185 to 250 µm fraction of this sample compared to the finer three fractions. The less than 64 µm fraction has the highest abundance of gahnite (0.103) in the single up-ice sample (09-MPB-060). Corundum is present in all samples, with values ranging from 0.103 to 2.852 normalized grains per 1000 grains. The highest abundances by far (0.766–2.852) are in the four fractions of sample 09-MPB-058; Corundum is most abundant in the 185 to

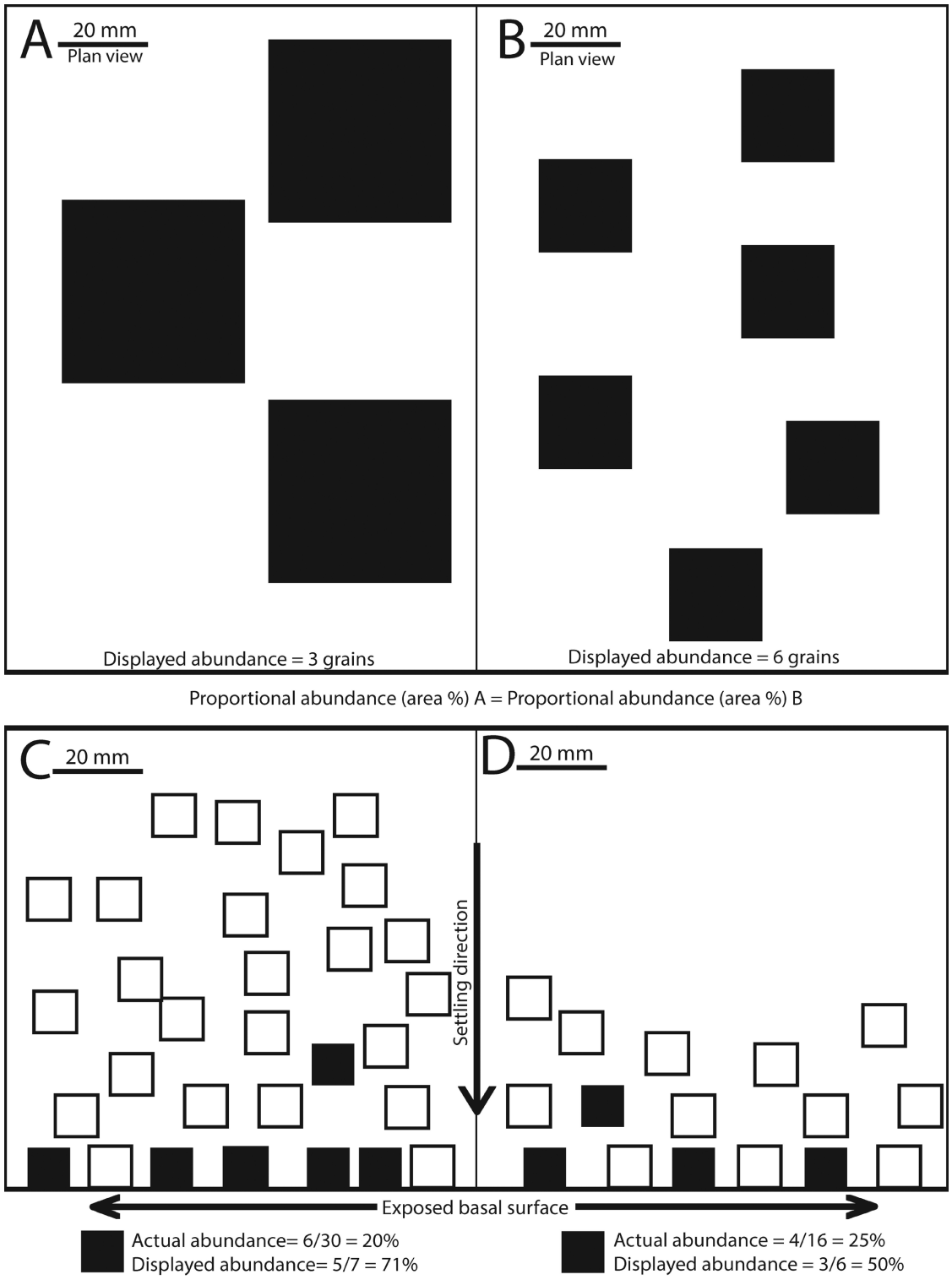

Figure 5. Conceptual views of epoxy grain mounts illustrating the importance of combining grain counts and proportion coverage (area per cent) to determine mineral abundance. The proportion of the basal surface covered by heavy grains (black squares) in the epoxy grain mounts A and B is identical, even though mount A contains three large mineral grains and B contains six small grains. In this scenario, grain counts alone imply that the mineral of interest is more abundant in mount B than in mount A, when in fact it is equally abundant. The cross-sections through epoxy grain mounts C and D show heavier (solid black) mineral grains settling preferentially through the curing epoxy. Grain mount C contains 30 grains total, with four black grains out of seven grains exposed on the basal surface; grain mount D contains fewer grains (16) than mount C, and has three black grains out of six grains exposed on the basal surface. The actual abundance of heavy (black) grains per total grains mounted in epoxy is lower in mount C (5 out of 30 grains vs. 4 out of 16 grains) than in mount D, but due to the preferential settling of heavier minerals through the curing epoxy, the displayed abundance on the polished basal surface is higher in mount C (71%) than D (50%).

Table 3. Abundance of selected ore minerals in four till samples located up and down ice of the Izok Lake volcanogenic massive-sulfide deposit. Mineral-abundance data are reported as the number of indicator mineral grains per total grains, normalized to 1000 grains and the 2-D proportion (area per cent) of the polished mount surface that each mineral takes up. Grain counts from the 250 to 500 µm heavy-mineral fraction of the same samples, obtained by visual grain picking, have been normalized to a 10 kg sample mass (data *after* Hicken et al., 2013b).

Sample number	Distance from mineralization	Size fraction (µm)	Chalcopyrite		Galena		Pyrite		Sphalerite	
			Grain count (norm.)	Proportion (area %)	Grain count (norm.)	Proportion (area %)	Grain count (norm.)	Proportion (area %)	Grain count (norm.)	Proportion (area %)
09-MPB-060	1 km up ice	185–250	0.00	0.0000	0.07	0.0001	0.51	0.0001	0.00	0.0000
		125–185	0.00	0.0000	0.00	0.0000	0.24	0.0009	0.00	0.0000
		64–125	0.00	0.0000	0.00	0.0000	0.40	0.0015	0.00	0.0000
		<64	0.02	0.0001	0.00	0.0000	0.06	0.0014	0.00	0.0000
		250–500	0	NA	0	NA	0	NA	0	NA
09-MPB-058	0.5 km down ice	185–250	0.40	0.0006	0.40	0.0002	2.50	0.2117	8.09	0.8045
		125–185	0.27	0.0177	0.09	0.0001	2.41	0.1592	1.50	0.4314
		64–125	0.21	0.0010	0.03	0.0001	1.11	0.0966	1.14	0.1523
		<64	0.07	0.0044	0.00	0.0000	0.25	0.0151	0.60	0.0710
		250–500	9	NA	0	NA	339	NA	1271	NA
09-MPB-075	2.5 km down ice	185–250	0.05	0.0002	0.29	0.0004	0.49	0.0019	0.00	0.0000
		125–185	0.15	0.0004	0.00	0.0000	0.19	0.0012	0.00	0.0000
		64–125	0.00	0.0000	0.09	0.0001	0.12	0.0011	0.00	0.0000
		<64	0.06	0.0001	0.00	0.0000	0.17	0.0017	0.00	0.0000
		250–500	0	NA	0	NA	0	NA	0	NA
12-MPB-902	8 km down ice	185–250	0.09	0.0001	0.22	0.0006	0.26	0.0007	0.00	0.0000
		125–185	0.12	0.0001	0.00	0.0000	0.40	0.0013	0.08	0.0001
		64–125	0.05	0.0000	0.03	0.0004	0.08	0.0004	0.00	0.0000
		<64	0.03	0.0000	0.00	0.0000	0.07	0.0004	0.03	0.0001
		250–500	0	NA	0	NA	0	NA	0	NA

NA = not applicable
norm.: normalized

Table 4. Abundance of selected alteration minerals in four till samples located up and down ice of the Izok Lake volcanogenic massive-sulfide deposit. Mineral-abundance data are reported as the number of indicator mineral grains per total grains, normalized to 1000 grains and the 2-D proportion (area per cent) of the polished mount surface that each mineral takes up. Grain counts for the 250 to 500 µm heavy-mineral fraction of the same samples, obtained by visual grain picking, have been normalized to a 10 kg sample mass (data *after* Hicken et al., 2013b).

Sample number	Distance from mineralization	Size fraction (µm)	Corundum		Epidote		Staurolite		Gahnite	
			Grain count (norm.)	Proportion (area %)	Grain count (norm.)	Proportion (area %)	Grain count (norm.)	Proportion (area %)	Grain count (norm.)	Proportion (area %)
09-MPB-060	1 km up ice	185–250	0.14	0.0024	21.23	5.4712	13.57	3.1242	0.00	0.0000
		125–185	0.69	0.0335	29.28	6.0791	11.41	2.6086	0.08	0.0283
		64–125	0.61	0.0553	48.06	8.9677	12.73	2.2661	0.03	0.0000
		<64	0.81	0.0366	47.26	7.2992	13.99	1.9695	0.10	0.0064
		250–500	NA	NA	602*	NA	3061**	NA	0**	NA
09-MPB-058	0.5 km down ice	185–250	3.59	0.1770	26.65	6.7352	12.68	2.0104	2.30	0.3724
		125–185	1.00	0.0582	39.24	8.6277	10.57	2.4334	1.55	0.0743
		64–125	1.07	0.1177	59.23	9.2708	13.24	1.9613	0.90	0.1059
		<64	0.87	0.0383	61.71	8.6900	16.21	1.9937	1.14	0.1309
		250–500	NA	NA	1825*	NA	2542**	NA	77**	NA
09-MPB-075	2.5 km down ice	185–250	0.24	0.0353	22.09	7.2143	6.56	1.6389	1.03	0.1854
		125–185	0.41	0.0050	27.03	6.4038	5.62	1.6028	0.34	0.0444
		64–125	0.68	0.0399	48.04	9.3994	8.50	1.4065	1.05	0.1107
		<64	0.27	0.0269	42.82	6.7296	8.95	1.2080	1.11	0.1458
		250–500	NA	NA	2678*	NA	971**	NA	64**	NA
12-MPB-902	8 km down ice	185–250	0.30	0.0065	14.40	4.1317	5.18	1.8300	0.35	0.0462
		125–185	0.32	0.0094	22.55	5.3092	5.83	1.3816	0.83	0.2069
		64–125	0.32	0.0225	32.15	6.1219	7.35	1.3350	0.56	0.0831
		<64	0.30	0.0205	33.24	4.1088	7.83	0.8659	0.85	0.1128
		250–500	NA	NA	633*	NA	1634**	NA	24**	NA

*Geological Survey of Canada, unpublished data
**Hicken et. al (2013b)
NA = not applicable
norm.: normalized

Table 5. The proportion (area per cent) of each ore mineral in till samples from the Izok Lake deposit, Nunavut, present as liberated grains or as a component of a composite particle.

		Size	Chalcopyrite		Galena		Pyrite		Pyrrhotite		Sphalerite	
Sample number	Distance from mineralization	fraction (µm)	Liberated (area %)	Composite (area %)	Liberated (area %)	Composite (area %)	Liberated (area %)	Composite (area %)	Liberated (area %)	Composite (area %)	Liberated (area %)	Composite (area %)
09-MPB-060	1 km up ice	185–250	0.00	0.00	0.00	100.00	0.00	100.00	0.00	100.00	0.00	0.00
		125–185	0.00	0.00	0.00	0.00	0.00	100.00	0.00	100.00	0.00	0.00
		64–125	0.00	0.00	0.00	0.00	0.00	100.00	0.00	100.00	0.00	0.00
		<64	0.00	0.00	0.00	0.00	0.00	100.00	0.00	100.00	0.00	0.00
09-MPB-058	0.5 km down ice	185–250	55.86	44.14	0.00	100.00	0.00	100.00	0.00	100.00	82.72	17.28
		125–185	96.43	3.57	0.00	100.00	2.86	97.14	0.00	100.00	66.91	33.09
		64–125	0.00	100.00	0.00	100.00	14.29	85.71	0.00	100.00	37.58	62.42
		<64	93.68	6.32	0.00	0.00	15.01	84.99	86.56	13.44	96.71	3.29
09-MPB-075	2.5 km down ice	185–250	0.00	100.00	45.05	54.95	0.00	100.00	0.00	100.00	0.00	0.00
		125–185	0.00	100.00	0.00	0.00	0.00	100.00	0.00	100.00	0.00	0.00
		64–125	0.00	0.00	0.00	100.00	0.00	100.00	0.00	100.00	0.00	0.00
		<64	0.00	100.00	0.00	0.00	0.00	100.00	0.00	100.00	0.00	0.00
12-MPB-902	8 km down ice	185–250	0.00	100.00	35.09	64.91	0.00	100.00	0.00	100.00	0.00	0.00
		125–185	0.00	100.00	0.00	0.00	0.00	100.00	0.00	100.00	0.00	100.00
		64–125	0.00	100.00	100.00	0.00	0.00	100.00	0.00	100.00	0.00	0.00
		<64	0.00	100.00	0.00	0.00	0.00	0.00	0.00	100.00	0.00	100.00

Contents

Table 6. Abundance of ore and related indicator minerals in five till samples collected up ice, overlying, and down ice of the Sisson granite-hosted W-Mo deposit, New Brunswick.

Sample number	Distance from mineralizatio	Size fraction (µm)	Arsenopyrite		Pyrite		Sphalerite		Chalcopyrite		Galena	
			Grain count (norm.)	Proportion (area %)	Grain count (norm.)	Proportion (area %)	Grain count (norm.)	Proportion (area %)	Grain count (norm.)	Proportion (area %)	Grain count (norm.)	Proportion (area %)
11-MPB-520	Up iceBackground	185–250	0.0000	0.00	0.2590	0.01	0.0000	0.00	0.0432	0.00	0.0000	0.00
		125–185	0.0000	0.00	0.2413	0.00	0.0000	0.00	0.0268	0.00	0.0000	0.00
		64–125	0.0000	0.00	0.1401	0.00	0.0467	0.00	0.0000	0.00	0.0000	0.00
		<64	0.0000	0.00	0.0498	0.00	0.0000	0.00	0.0000	0.00	0.0000	0.00
		250–500*	0	NA	0	NA	0	NA	0	NA	0	NA
11-MPB-505	Ellipse Overlying	185–250	0.0000	0.00	0.4156	0.00	0.0416	0.00	0.0000	0.00	0.0000	0.00
		125–185	0.0333	0.00	0.3619	0.00	0.0095	0.00	0.0857	0.00	0.0286	0.00
		64–125	0.0190	0.00	0.3941	0.00	0.0142	0.00	0.0617	0.00	0.0285	0.00
		<64	0.0000	0.00	0.1667	0.00	0.0167	0.00	0.0000	0.00	0.0000	0.00
		250–500*	0	NA	0	NA	0	NA	1	NA	0	NA
11-MPB-567	Zone III Overlying	185–250	0.4436	0.18	15.8808	0.94	0.0444	0.00	0.9759	0.01	0.0000	0.00
		125–185	0.3359	0.12	5.6792	0.39	0.0234	0.00	0.6640	0.02	0.1719	0.02
		64–125	0.2377	0.05	3.5922	0.31	0.0053	0.00	0.0792	0.00	0.2113	0.04
		<64	0.4258	0.05	3.1054	0.32	0.0156	0.00	0.0469	0.00	0.5547	0.06
		250–500*	0	NA	217	NA	0	NA	8	NA	0	NA
11-MPB-525	4 km Down ice	185–250	0.0000	0.00	0.9090	0.00	0.0000	0.00	0.0000	0.00	0.1515	0.00
		125–185	0.0207	0.01	0.4766	0.00	0.0345	0.00	0.1174	0.00	0.0000	0.00
		64–125	0.0154	0.00	0.2819	0.00	0.0103	0.00	0.0923	0.00	0.0000	0.00
		<64	0.0035	0.00	0.1633	0.00	0.0069	0.00	0.0625	0.00	0.0000	0.00
		250–500*	0	NA	0	NA	0	NA	0	NA	0	NA
11-MPB-539	10 km Down ice	185–250	0.0000	0.00	1.0131	0.01	0.0563	0.00	0.1126	0.00	0.1689	0.00
		125–185	0.0661	0.00	0.9011	0.00	0.0909	0.00	0.4547	0.00	0.0000	0.00
		64–125	0.0000	0.00	0.3634	0.00	0.0058	0.00	0.0173	0.00	0.0173	0.00
		<64	0.0000	0.00	0.1913	0.00	0.0042	0.00	0.0166	0.00	0.0083	0.00
		250–500*	0	NA	0	NA	0	NA	0	NA	0	NA

*McClenaghan et al. (2013a)
NA: not applicable
norm.: normalized
Mineral-abundance data are reported as the number of indicator mineral grains per total grains, normalized to 1000 grains and the 2-D proportion (area per cent) of the polished mount surface that each mineral takes up.
Grain counts from the 250 to 500 µm heavy-mineral fraction of the same samples, obtained by visual grain picking, have been normalized to a 10 kg sample mass (data *after* McClenaghan et al., 2013a).

Table 7. Abundance of sulfide indicator minerals in five till samples up and down ice of the Sisson deposit.

Sample number	Distance from mineralization	Size fraction (µm)	Scheelite		Wolframite		Molybdenite		Bismuth minerals	
			Grain count (norm.)	Proportion (area %)	Grain count (norm.)	Proportion (area %)	Grain count (norm.)	Proportion (area %)	Grain count (norm.)	Proportion (area %)
11-MPB-520	Up ice Background	185–250	0.0000	0.00	0.0000	0.00	0.0000	0.00	0.0000	0.00
		125–185	0.0000	0.00	0.0000	0.00	0.0000	0.00	0.0000	0.00
		64–125	0.0000	0.00	0.0000	0.00	0.0000	0.00	0.0000	0.00
		<64	0.0000	0.00	0.0000	0.00	0.0000	0.00	0.0166	0.00
		250–500*	0	NA	0	NA	0	NA	0	NA
11-MPB-505	Ellipse Overlying	185–250	5.2365	1.96	0.4987	0.02	0.0000	0.00	0.0416	0.00
		125–185	1.5048	0.35	0.2714	0.02	0.0048	0.00	0.0286	0.00
		64–125	1.4911	0.36	0.2279	0.01	0.0047	0.00	0.0332	0.00
		<64	4.1512	0.50	0.1500	0.03	0.0000	0.00	0.0667	0.00
		250–500*	515	NA	0	NA	0	NA	0	NA
11-MPB-567	Zone III Overlying	185–250	3.9037	1.59	1.1977	0.05	0.3549	0.10	0.0000	0.00
		125–185	1.9061	1.18	0.1484	0.02	0.4218	0.17	0.2969	0.00
		64–125	4.3159	1.21	0.2694	0.03	0.4068	0.10	0.1426	0.00
		<64	10.2850	1.33	0.3945	0.03	0.1445	0.02	0.2031	0.02
		250–500*	261	NA	0	NA	87	NA	2	NA
11-MPB-525	4 km Down ice	185–250	0.4040	0.08	0.0505	0.07	0.0000	0.00	0.0000	0.00
		125–185	0.0967	0.02	0.0138	0.01	0.0000	0.00	0.1243	0.00
		64–125	0.0256	0.00	0.0103	0.00	0.0000	0.00	0.0820	0.00
		<64	0.0521	0.00	0.0764	0.01	0.0000	0.00	0.0764	0.01
		250–500*	8	NA	0	NA	0	NA	0	NA
4 kmDown ice	10 km Down ice	185–250	0.0000	0.00	0.1689	0.10	0.0000	0.00	0.0000	0.00
		125–185	0.0661	0.01	0.0413	0.03	0.0000	0.00	0.3555	0.01
		64–125	0.0404	0.00	0.1327	0.02	0.0000	0.00	0.0462	0.00
		<64	0.0582	0.00	0.1539	0.02	0.0000	0.00	0.0749	0.00
		250–500*	7	NA	0	NA	0	NA	0	NA

*McClenaghan et al. (2013a)
NA: not applicable
norm.: normalized
Mineral-abundance data are reported as the number of indicator mineral grains per total grains, normalized to 1000 grains and the 2-D proportion (area per cent) of the polished mount surface that each mineral takes up.
Grain counts from the 250 to 500 µm heavy-mineral fraction of the same samples, obtained by visual grain picking, have been normalized to a 10 kg sample mass (data *after* McClenaghan et al., 2013a).

Contents

Table 8. The proportion (area per cent) of ore and sulfide minerals in till samples from the Sisson deposit, New Brunswick, present as either liberated grains or as a component of a composite particle.

		Size	Arsenopyrite		Chalcopyrite		Galena		Pyrite		Sphalerite	
Sample number	Distance from mineralization	Fraction (µm)	Liberated (area %)	Composite area (%)	Liberated (area %)	Composite area (%)	Liberated (area %)	Composite area (%)	Liberated (area %)	Composite area (%)	Liberated (area %)	Composite area (%)
11-MPB-520	Up ice Background	185–250	0.00	0.00	0.00	100.00	0.00	0.00	0.00	100.00	0.00	0.00
		125–185	0.00	0.00	0.00	100.00	0.00	0.00	0.00	100.00	0.00	0.00
		64–125	0.00	0.00	0.00	0.00	0.00	0.00	0.00	100.00	0.00	100.00
		<64	0.00	0.00	0.00	0.00	0.00	0.00	0.00	100.00	0.00	0.00
11-MPB-505	Ellipse Overlying	185–250	0.00	0.00	0.00	0.00	0.00	0.00	0.00	100.00	0.00	100.00
		125–185	0.00	100.00	0.00	100.00	0.00	100.00	0.00	100.00	0.00	100.00
		64–125	0.00	100.00	0.00	100.00	0.00	100.00	0.00	100.00	0.00	100.00
		<64	0.00	0.00	0.00	0.00	0.00	0.00	0.00	100.00	0.00	100.00
11-MPB-567	Zone III Overlying	185–250	0.30	99.70	0.00	100.00	0.00	0.00	13.04	86.96	0.00	100.00
		125–185	49.04	50.96	62.32	37.68	52.44	47.56	24.78	75.22	0.00	100.00
		64–125	73.85	26.15	54.89	45.11	27.96	72.04	41.40	58.60	0.00	100.00
		<64	85.67	14.33	75.53	24.47	58.36	41.64	66.13	33.87	98.27	1.73
11-MPB-525	4 km Down ice	185–250	0.00	0.00	0.00	0.00	51.43	48.57	0.00	100.00	0.00	0.00
		125–185	0.00	100.00	0.00	100.00	0.00	0.00	0.00	100.00	0.00	100.00
		64–125	0.00	100.00	0.00	100.00	0.00	0.00	0.00	100.00	0.00	100.00
		<64	0.00	100.00	0.00	100.00	0.00	0.00	0.00	100.00	0.00	100.00
11-MPB-539	10 km Down ice	185–250	0.00	0.00	0.00	100.00	11.29	88.71	0.00	100.00	0.00	100.00
		125–185	0.00	100.00	0.00	100.00	0.00	0.00	2.31	97.69	0.00	100.00
		64–125	0.00	0.00	0.00	100.00	0.00	100.00	0.00	100.00	0.00	100.00
		<64	0.00	0.00	0.00	100.00	0.00	100.00	58.98	41.02	0.00	100.00

Table 8. (cont.) The proportion (area per cent) of ore and sulfide minerals in till samples from the Sisson deposit, New Brunswick, present as either liberated grains or as a component of a composite particle.

		Size	Scheelite		Wolframite		Molybdenite		Bismuth minerals	
Sample number	Distance from mineralization	Fraction (µm)	Liberated (area %)	Composite area (%)	Liberated (area %)	Composite area (%)	Liberated (area %)	Composite area (%)	Liberated (area %)	Composite area (%)
11-MPB-520	Up ice Background	185–250	0.00	0.00	0.00	0.00	0.00	0.00	0.00	0.00
		125–185	0.00	0.00	0.00	0.00	0.00	0.00	0.00	0.00
		64–125	0.00	0.00	0.00	0.00	0.00	0.00	0.00	0.00
		<64	0.00	0.00	0.00	0.00	0.00	0.00	100.00	0.00
11-MPB-505	Ellipse Overlying	185–250	98.04	1.96	95.17	4.83	0.00	0.00	0.00	100.00
		125–185	44.25	55.75	49.90	50.10	0.00	100.00	0.00	100.00
		64–125	44.70	55.30	46.44	53.56	0.00	100.00	0.00	100.00
		<64	96.17	3.83	21.37	78.63	0.00	0.00	0.00	100.00
11-MPB-567	Zone III Overlying	185–250	78.48	21.52	11.51	88.49	99.44	0.56	0.00	0.00
		125–185	64.21	35.79	92.32	7.68	15.85	84.15	0.00	100.00
		64–125	88.41	11.59	82.80	17.20	73.74	26.26	38.73	61.27
		<64	81.67	18.33	46.01	53.99	74.66	25.34	63.30	36.70
11-MPB-525	4 km Down ice	185–250	95.82	4.18	0.00	0.00	0.00	0.00	0.00	0.00
		125–185	10.64	89.36	0.00	100.00	0.00	0.00	0.00	100.00
		64–125	87.25	12.75	0.00	100.00	0.00	0.00	0.00	100.00
		<64	52.33	47.67	0.00	0.00	0.00	0.00	45.22	54.78
11-MPB-539	10 km Down ice	185–250	0.00	0.00	0.00	0.00	0.00	0.00	0.00	0.00
		125–185	55.27	44.73	0.00	0.00	0.00	0.00	0.00	100.00
		64–125	96.46	3.54	0.00	0.00	0.00	0.00	89.35	10.65
		<64	92.90	7.10	0.00	100.00	0.00	0.00	68.14	31.86

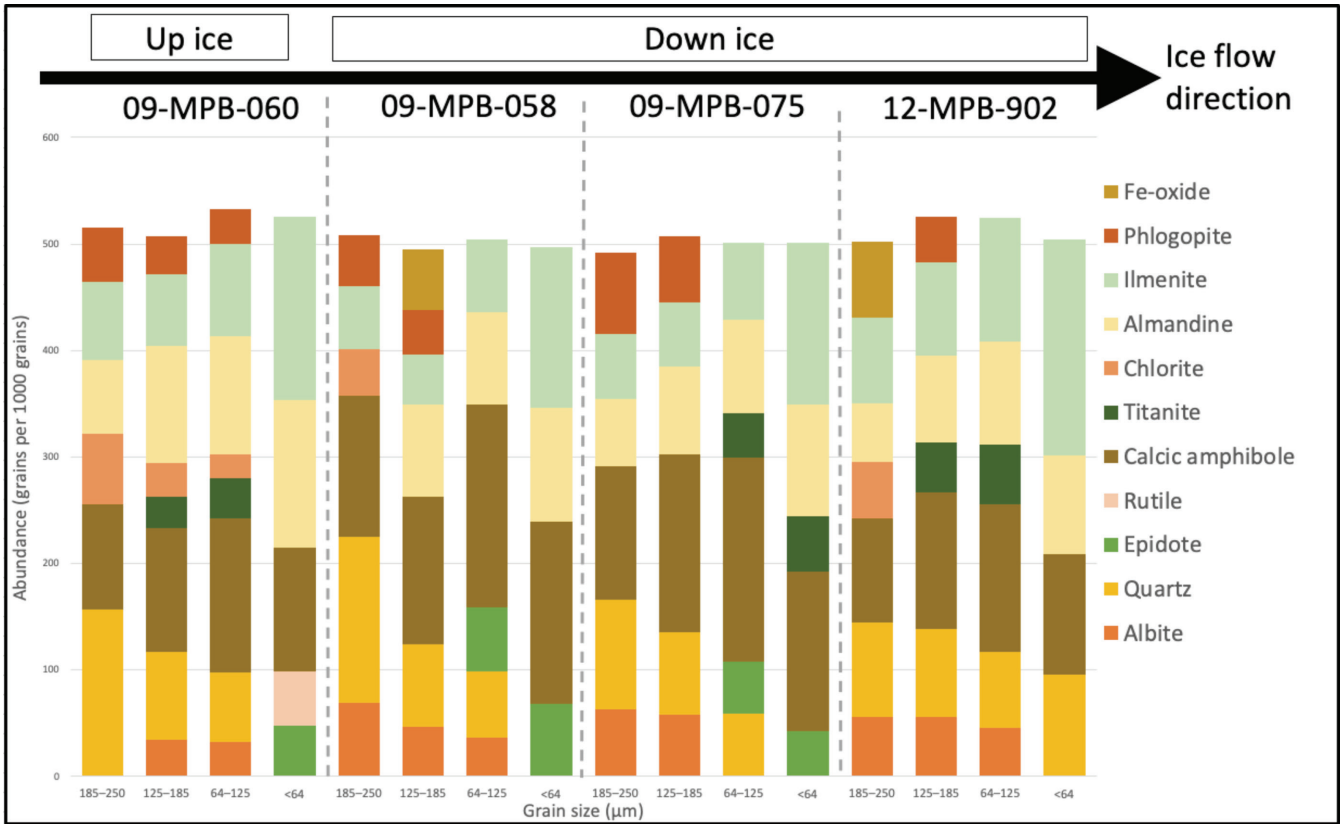

Figure 6. Mineral abundance (normalized to grains per 1000 grains) for the most abundant minerals comprising 50% of the less than 250 µm fraction of till heavy-mineral concentrates, for the 185 to 250, 125 to 185, 64 to 125, and less than 64 µm fractions of four till samples from the Izok Lake deposit, Nunavut. The black arrow denotes the direction of ice flow. Sample locations relative to mineralization: 09-MPB-060: 1 km up ice; 09-MPB-058: 0.5 km down ice; 09-MPB-075: 2.5 km down ice; and 12-MPB-902: 8 km down ice.

250 µm fraction of this sample. The fewest grains of corundum (0.103) are detected in the 185 to 250 µm fraction of sample 09-MPB-060, located 1 km up ice of the deposit.

Corundum occurs as discrete and composite grains, with the latter consisting of gahnite, hercynite, chlorite, garnet, and Fe-oxide minerals. Grains consisting of gahnite-corundum intergrowths are observed in all of the down-ice till samples, but only sample 09-MPB-058 has gahnite-corundum intergrowths in the 185 to 250 µm fraction. Corundum from proximal down-ice sample 09-MPB-058 also contains inclusions of the ore minerals galena and chalcopyrite within discrete grains and grains intergrown with gahnite.

Staurolite abundance ranges from 5.143 to 16.629 normalized grains per 1000 grains. It is present in all four size fractions of all four samples. The highest abundance of staurolite (16.629) is in sample 09-MPB-058. The less than 64 µm fraction of all four samples consistently has the highest abundance of staurolite. In general, staurolite content in till decreases as distance down ice increases.

Epidote abundance ranges from 14.478 to 68.469 normalized grains per 1000 grains and it is identified in all four size fractions of all four samples. The less than 64 µm fraction of sample 09-MPB-058 contains the most epidote (68.469); the lowest abundance is detected in the 185 to 250 µm fraction of distal down-ice sample 12-MPB-902 (8 km down ice). The greatest abundance of epidote grains is in the 64 to 125 µm or less than 64 µm fraction of all samples.

Total Fe-oxide mineral abundance ranges from 14.886 to 71.697 normalized grains per 1000 grains and Fe-oxide minerals are identified in all four size fractions of all four samples. The 185 to 250 µm fraction of sample 12-MPB-902 contains the most Fe-oxide mineral grains (71.697). The lowest abundance is detected in the 125 to 185 µm fraction of sample 09-MPB-075, located 3 km down ice of mineralization.

Sulfide ore minerals

Sulfide ore minerals are present in the samples as discrete, liberated grains and as components of composite mineral particles. The proportion (area per cent) of each ore mineral contained as liberated grains or as part of composite particles is reported in Table 5.

Chalcopyrite is predominantly present as inclusions in grains of other, more oxidation-resistant minerals (Fig. 7a–d, Table 3) such as epidote, calcic amphibole, garnet, and Fe-oxide minerals. Chalcopyrite abundance (discrete grains and inclusions) ranges from 0.021 to 0.503 normalized grains per 1000 grains and occurs in all four fractions of two of the three down-ice samples, and all except the 64 to 125 µm fraction of the third sample. It is most abundant (0.503) in sample 09-MPB-058 and is present in all four size fractions of the sample: the 185 to 250 µm fraction has the most grains and the less than 64 µm fraction the least. In up-ice sample 09-MPB-060, chalcopyrite is only identified in very low abundance (0.021) in the less than 64 µm fraction. Sphalerite is the least abundant of the five main sulfide minerals reported here, despite being much more abundant than chalcopyrite in the Izok Lake deposit itself. Sphalerite is less abundant in till samples compared to chalcopyrite because sphalerite is more susceptible to postglacial oxidation than chalcopyrite (Averill, 2001). Sphalerite is only present in two samples, with values ranging from 0.033 to 7.214 normalized grains per 1000 grains. It is present in all four size fractions of sample 09-MPB-058 and in two size

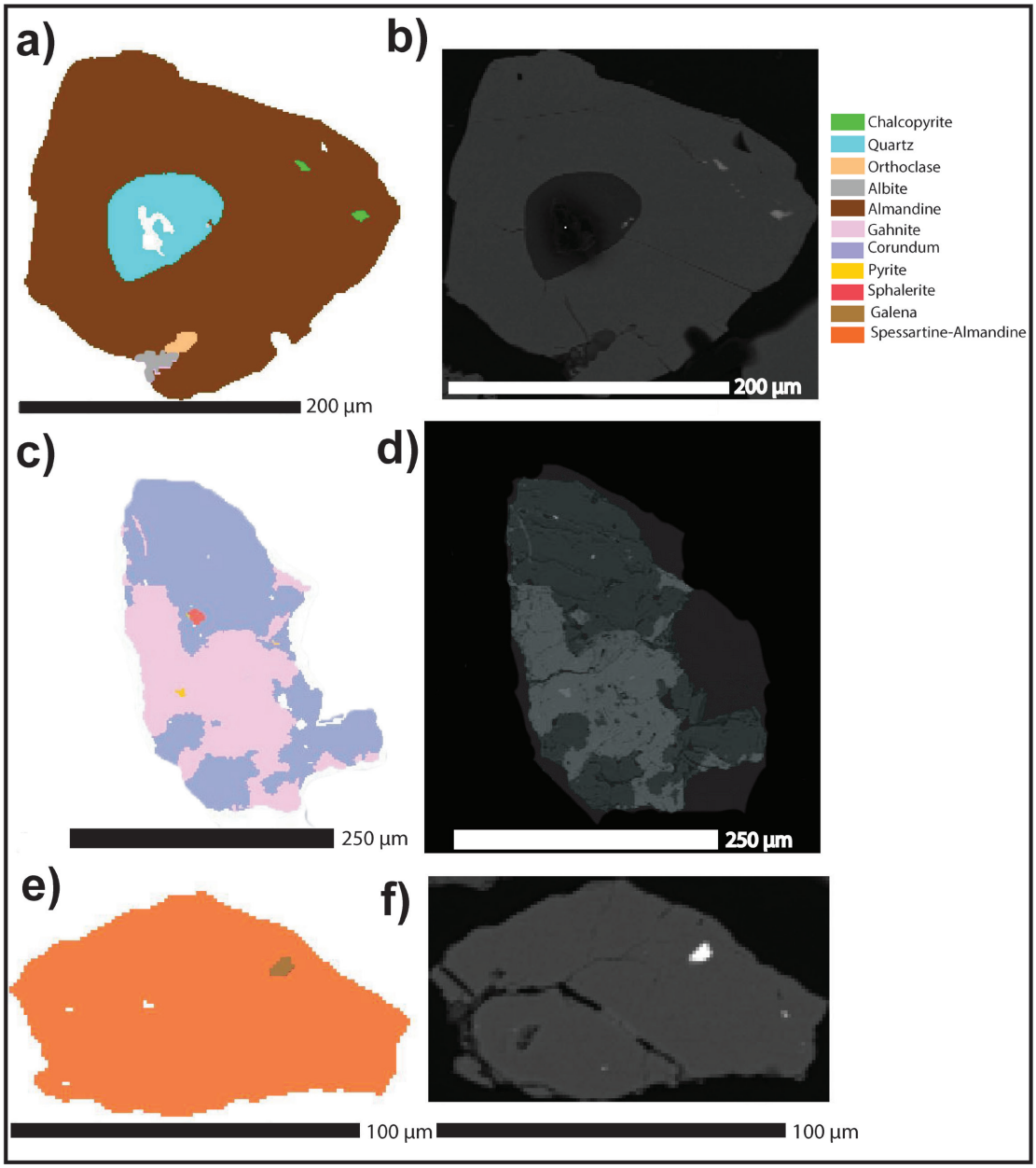

Figure 7. False-colour mineral-liberation analysis (MLA) and backscatter emission (BSE) images of mineral grains from till at the Izok Lake deposit, Nunavut: **a)** MLA and **b)** BSE images of chalcopyrite inclusions in almandine; **c)** MLA and **d)** images of intergrown gahnite and corundum; **e)** MLA and **f)** BSE images of galena inclusion in garnet. Scale bars below images vary.

fractions (125–185 µm and <64 µm) of sample 12-MPB-902. In sample 09-MPB-058, it is most abundant in the 185 to 250 µm fraction and least abundant in the less than 64 µm fraction. No sphalerite is detected in the up-ice sample. Sphalerite is present as discrete grains and as inclusions in other minerals.

Galena (Fig. 7e, f) is present in all four samples as very small inclusions (0.027–0.499 normalized grains per 1000 grains) in larger grains of more oxidation-resistant minerals such as chlorite, calcic amphibole, and garnet. It is most abundant overall in sample 09-MPB-058, and the 185 to 250 µm fraction has the greatest abundance in each sample.

Pyrrhotite is primarily present as inclusions in other minerals, including calcic amphibole, garnet, Fe-oxide minerals, and other sulfide ore minerals. One discrete grain of pyrrhotite is present in the less than 64 µm fraction of sample 09-MPB-058. Pyrrhotite abundance (discrete grains and inclusions) ranges from 0.070 to 1.000 normalized grains per 1000 grains. It is most abundant in sample 09-MPB-058, where the highest abundance occurs in the 125 to 185 µm fraction. It is present in all size fractions of all samples, with the highest abundances occurring in the 185 to 250 and 125 to 185 µm fractions. Pyrite is present in all four size fractions of all four samples, occurring as discrete grains and as inclusions in other grains. Some grains containing pyrite inclusions also contain inclusions of chalcopyrite and pyrrhotite. Total pyrite abundance (discrete grains and inclusions) varies between 0.066 and 3.691 normalized grains per 1000 grains. Abundance is highest in sample 09-MPB-058, where it is most abundant (3.691) in the 185 to 250 µm size fraction and least abundant (0.469) in the less than 64 µm size fraction. Pyrite abundance in samples 09-MPB-075 and 12-MPB-902, located 3 and 8 km down ice of mineralization, respectively, is lower than in sample 09-MPB-060, located 1 km up ice of mineralization.

Sisson

Figure 8 charts the most abundant minerals identified in each size fraction of each sample, which together comprise 50% of the minerals present in the Sisson deposit samples. They include calcic amphibole, titanite, rutile, quartz, and biotite. Tables 6 and 7 detail the abundance of key ore and alteration indicator minerals at each site. Figure 8 indicates that unknown minerals (those for which a suitable spectral match was not found in the MLA mineral reference library)

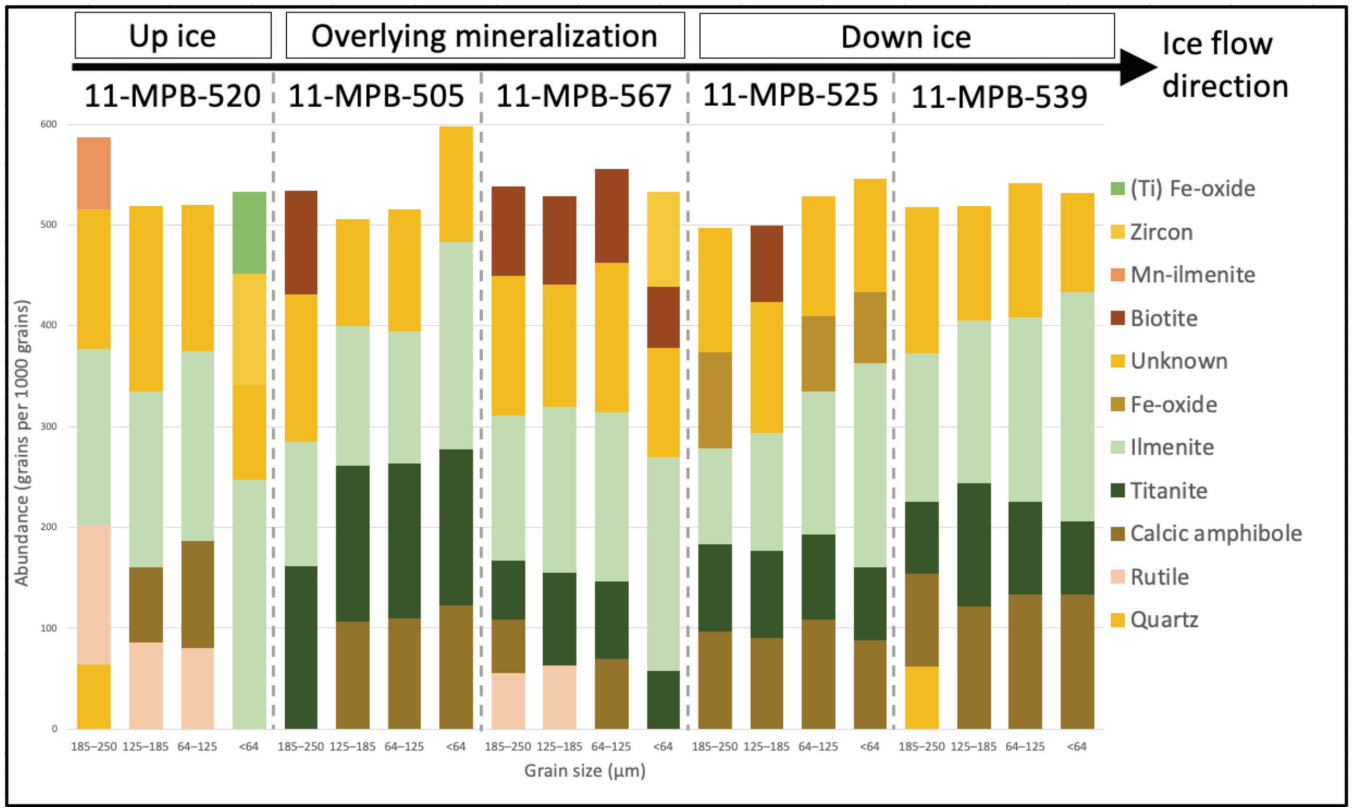

Figure 8. Mineral abundance (normalized to grains per 1000 grains) for the most abundant minerals comprising 50% of the less than 250 µm fraction of till heavy-mineral concentrates, for the 185 to 250, 125 to 185, 64 to 125, and less than 64 µm fractions of five till samples from the Sisson granite-hosted W-Mo deposit, New Brunswick. Labels above denote the position of each sample relative to massive-sulfide mineralization, and the black arrow denotes the direction of ice flow. Sample locations relative to mineralization: 11-MPB-520: 4 km up ice; 11-MPB-567 and 11-MPB-505: overlying mineralization; 11-MPB-525: 4 km down ice; 11-MPB-539: 10 km down ice.

represent a large portion of each sample. Additional examination of these unknown minerals using a combination of SEM-EDS and EPMA is needed to identify the mineralogy of the 'unknown' grains. Biotite, titanite, and Fe-oxide minerals are all present in greater proportional abundance in till from sites overlying and down ice of mineralization (11-MPB-505, 11-MPB-567, 11-MPB-525, and 11-MPB-539) than in up-ice sample 11-MPB-520.

Ore minerals

Scheelite is present in varying amounts in the less than 250 µm HMC fraction of samples overlying and down ice of mineralization at the Sisson deposit (Table 7), as liberated and composite grains. The proportion of liberated and composite scheelite grains varies through the size fractions of each sample with no observable pattern (Table 8). No scheelite is identified in the less than 250 µm fraction of the up-ice sample 11-MPB-520. Scheelite is present in all size fractions examined (185–250 µm, 125–185 µm, 64–125 µm, and <64 µm) in samples 11-MPB-505, 11-MPB-567, and 11-MPB-525. Scheelite is not present in the 185 to 250 µm fraction of sample 11-MPB-539, the most distal down-ice sample, but is identified in the three finer size fractions. The highest abundance of scheelite (10.285 normalized grains per 1000 grains) occurs in the less than 64 µm fraction of sample 11-MPB-567, which overlies zone III mineralization.

Wolframite is present in varying amounts in samples overlying and down ice of mineralization (Table 6), and it occurs as liberated and composite grains (Table 8). Wolframite is present as both composite and liberated grains in the two samples (11-MPB-505 and 11-MPB-567) overlying mineralized zones (21.37–95.17% liberation), whereas in all down-ice samples it is only present in composite grains (0% liberation). Wolframite abundance is highest in samples 11-MPB-505 and 11-MPB-567 (0.148–0.3945 normalized grains per 1000 grains). In both down-ice samples, abundance decreases with increasing distance from mineralization.

Molybdenite is only present in samples 11-MPB-505 and 11-MPB-567 (Table 6), where it occurs as liberated and composite grains (Table 8). In sample 11-MPB-505, overlying Ellipse zone mineralization, molybdenite is only present in composite grains. In sample 11-MPB-567, overlying zone III mineralization, molybdenite is primarily present as liberated grains (73.74–99.44% liberation), except for the 125 to 185 µm fraction (15% liberation). The abundance of molybdenite is very low (0.005 normalized grains per 1000 grains) in till from sample 11-MPB-505, and greater (0.145–0.422 normalized grains per 1000 grains) in till from sample 11-MPB-567.

Accessory indicator minerals

Several bismuth minerals (bismuthinite, bismutite, joseite, and native bismuth) were previously identified visually (and confirmed by SEM) in the 250 to 2000 µm HMC fraction of Sisson bedrock, till, and stream-sediment samples by McClenaghan et al. (2013a, b, 2014b, 2015c, 2017b). Of the five samples examined in this study, only sample 11-MPB-567 was reported to contain bismuth minerals (2 grains/10 kg) in the 250 to 2000 µm HMC fraction (McClenaghan et al., 2013a). Of the identified bismuth minerals, only native bismuth is represented in the project mineral reference library; therefore, minerals containing bismuth as a significant component have a high likelihood of being classified as native bismuth.

Bismuth minerals are present in the less than 250 µm HMC fraction of all five till samples that we examined (McClenaghan et al., 2013a; Table 6), as liberated grains, composite grains, or both (Table 8). Bismuth minerals are only present in composite grains in the coarsest two size fractions (125–185 and 185–250 µm) that we examined, and discrete bismuth mineral grains (45.22–89.35 area per cent liberation) are observed in the less than 64 and 16 to 125 µm size fractions. The bismuth-bearing mineral identified in the up-ice sample (11-MPB-520) is only present as fully liberated grains. Bismuth abundance is highest in sample 11-MPB-567 (0.143–0.297 normalized grains per 1000 grains), which overlies zone III mineralization, with the exception of the 125 to 185 µm fraction of distal down-ice sample 11-MPB-539 (0.356 normalized grains per 1000 grains). A minor amount of bismuth mineral grains (0.017 normalized grains per 1000 grains) is identified in the less than 64 µm fraction of sample 11-MPB-520, the only fraction from that sample to contain bismuth minerals.

Chalcopyrite, arsenopyrite, sphalerite, pyrite, and galena grains were identified visually in the 250 to 2000 µm HMC fraction of bedrock, till, and stream-sediment samples from Sisson by McClenaghan et al. (2013a, 2014b, 2015c, 2017b); however, only chalcopyrite and pyrite were reported in the 250 to 2000 µm HMC fraction of the five till samples we examined in this study. The 250 to 500 µm fraction of till from sample 11-MPB-567, contained 8 grains of chalcopyrite per 10 kg and 217 grains of pyrite per 10 kg and the 500 to 2000 µm fraction contained 2 chalcopyrite grains per 10 kg. The 250 to 500 µm fraction of sample 11-MPB-505, overlying the Ellipse zone, contained 1 grain per 10 kg of chalcopyrite.

In our study, chalcopyrite abundance is highest (0.976 normalized grains per 1000 grains) in sample 11-MPB-567 (Table 7). Chalcopyrite abundance is lower (0.063–0.117 normalized grains per 1000 grains) in the proximal down-ice sample (11-MPB-525) but increases (0.017–0.454 normalized grains per 1000 grains) in the distal down-ice sample (11-MPB-539). Chalcopyrite abundance is 0.043 and

0.027 normalized grain per 1000 grains in the 185–250 µm and 125–185 µm fractions, respectively, of up-ice sample 11-MPB-520.

In our study, arsenopyrite is identified in the less than 250 µm fraction of all samples overlying and down ice of mineralization (Table 7). No arsenopyrite is identified in till up ice of mineralization (sample 11-MPB-520). Arsenopyrite abundance is highest in till from sample 11-MPB-567 (0.444 normalized grains per 1000 grains) and decreases in samples successively down ice (0.003–0.066 normalized grains per 1000 grains).

Pyrite is identified in the less than 250 µm fraction of all samples studied (Table 7). Pyrite abundance is highest (3.105–15.881 normalized grain per 1000 grains) in sample 11-MPB-567. The next highest abundance (0.191–1.01 normalized grains per 1000 grains) occurs in distal sample 11-MPB-539, followed by proximal till sample 11-MPB-525 (0.163–0.909 normalized grains per 1000 grains). The lowest abundance of pyrite (0.050–0.259 normalized grains per 1000 grains) is identified in up-ice sample 11-MPB-520.

Sphalerite is identified in the less than 250 µm fraction of all samples studied (Table 7). Sphalerite abundance is highest (0.004–0.056 normalized grains per 1000 grains) in distal down-ice sample 11-MPB-539, and occurs at 0.005 to 0.044 normalized grains per 1000 grains in fractions of the two samples overlying mineralization (11-MPB-505 and 11-MPB-567). Sphalerite is identified in one fraction (64–125 µm) of up-ice sample 11-MPB-520 (0.047 normalized grains per 1000 grains).

Galena is identified in samples overlying mineralization and down ice of the deposit (Table 7). It is most abundant in sample 11-MPB-567 (0.172–0.555 normalized grains per 1000 grains), with the highest abundance observed in the less than 64 µm fraction. In the two down-ice samples, galena is most abundant (0.152–0.169 normalized grains per 1000 grains) in the 185 to 250 µm fraction.

Sulfide minerals are primarily present as part of composite grains in all samples (Table 8), with the exception of sample 11-MPB-567, in which sulfide liberation ranges between 0 and 98.27%. Discrete grains of galena are identified in the 185 to 250 µm fraction of both down-ice samples, representing a transport distance of at least 10 km for liberated galena grains.

DISCUSSION

Izok Lake

Staurolite

Staurolite is a common metamorphic mineral in upper-amphibolite–facies terranes (Zaleski et al., 1991). Its presence in all four till samples from Izok Lake is expected because the deposit is in a terrane with a high metamorphic grade (Averill, 2001). Staurolite with significant Zn content (>5 weight percent) was identified as a useful marker in the exploration for metamorphosed VMS deposits, specifically as an intermediate mineral to form gahnite through the reaction of Zn-bearing biotite and staurolite during metamorphism (Stoddard, 1979; Dietvorst, 1981; Spry and Scott, 1986; Ghosh and Praveen, 2008); however, EPMA by Hicken (2012) of staurolite grains (n = 524) collected from the 250 to 2000 µm HMC fraction of till from Izok Lake identified very few grains containing greater than 5 weight per cent Zn. Spectra collected from these grains were included in our mineral reference library and Zn-rich staurolite is not observed in a significant abundance in our samples.

Gahnite

Hicken (2012) reported that gahnite ranges between 0.2 and 3.0 mm in size in bedrock polished thin sections (PTS) and between 0.25 and 1.0 mm in size in mineralized bedrock HMC. This size variation reflects the original grain size of the gahnite in bedrock that presented to the overriding glacier during the erosion of the deposit and the generation of till.

The pattern of gahnite abundance in the less than 250 µm fraction of till is similar to that reported by McClenaghan et al. (2015a) and Hicken et al. (2013b) for the 250 to 2000 µm fraction of till (Fig. 9). As gahnite grains were transported down ice they would have been comminuted with increasing transport distance, producing the pattern observed in our samples: decreasing abundance and size of gahnite in till with increasing distance down ice.

Hicken (2012) did not recover any gahnite from the 250 to 2000 µm HMC fraction of sample 09-MPB-060, located only 1 km up ice of the deposit; however, we found a few gahnite grains in the 125 to 185 and less than 64 µm fractions of the sample. It is possible that an alteration halo of the massive-sulfide mineralization containing fine-grained gahnite extends this far east. Alternatively, gahnite-rich bedrock may exist significantly farther up ice, as indicated by the presence of single grains of greater than 250 µm gahnite reported in till samples located 15 km up ice of the Izok Lake deposit (McClenaghan et al., 2012).

Corundum

Corundum is identified by Averill (2001) as an indicator mineral of metamorphosed VMS deposits and is intergrown with gahnite grains in till samples down ice of the Izok Lake deposit. The presence of corundum in association with gahnite has been reported at the Geco VMS deposit, Ontario, by Spry (1982) and is considered part of a mineral assemblage formed following high-grade metamorphism of chloritic precursor rocks (Theart et al., 2011). These chloritic

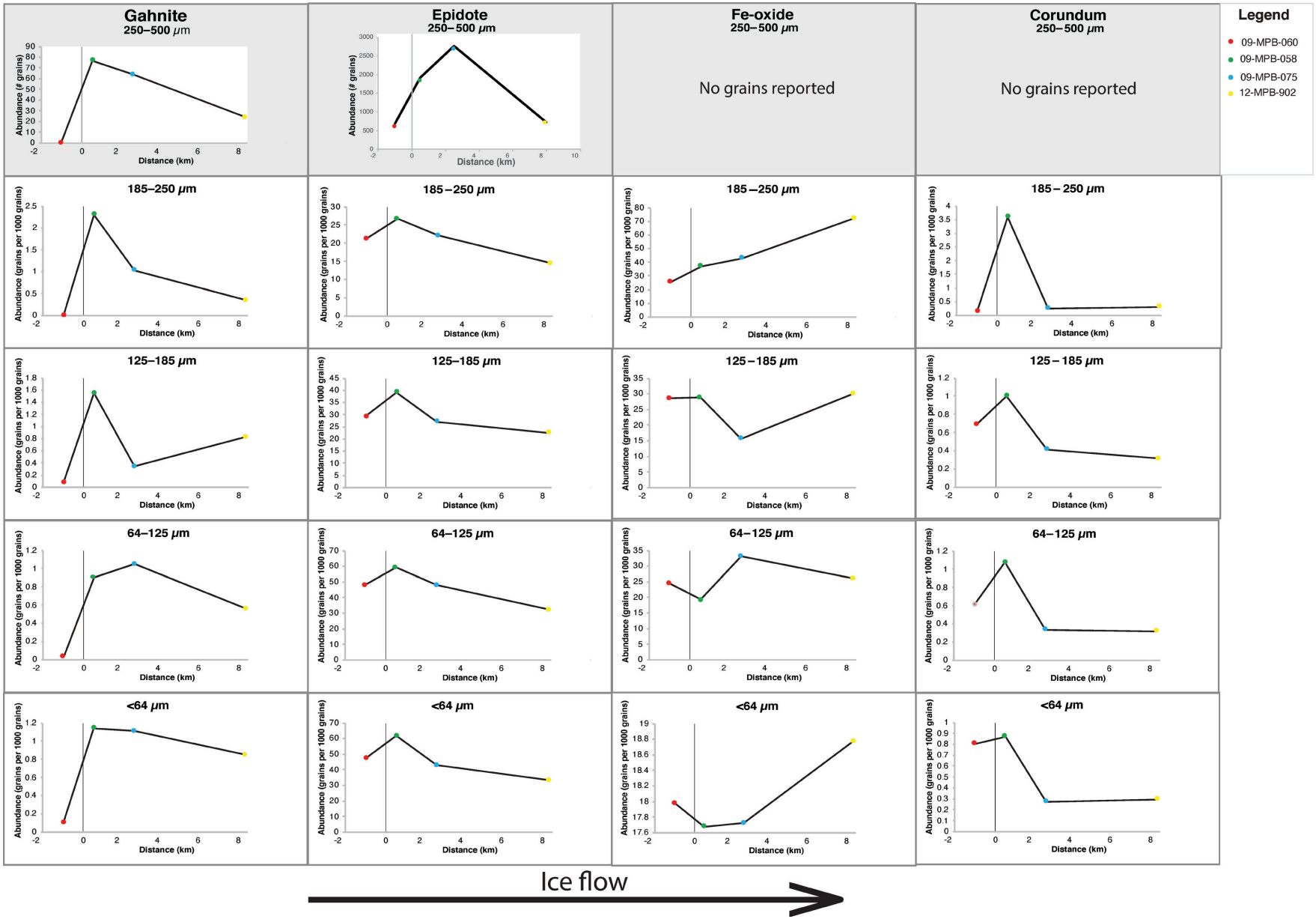

Figure 9. Alteration-mineral grain abundance in the 250 to 500 µm heavy-mineral concentrate (HMC) fraction (visual counts; Hicken et al., 2013b), and the 185 to 250, 125 to 185, 64 to 125, and less than 64 µm HMC fractions (MLA analysis; this study) of till samples from the Izok Lake deposit, Nunavut. Glacial transport distance is indicated by the black arrow, and the location of mineralization is indicated by a vertical grey line. Sample order, from up ice to distal down ice, is: 09-MPB-060 (1 km up ice), 09-MPB-058 (0.5 km down ice), 09-MPB-075 (2.5 km down ice), and 12-MPB-902 (8 km down ice).

precursor rocks are characteristic of the footwall hydrothermal alteration pipes of VMS deposits (Galley et al., 2007). At Izok Lake, Morrison (2004) identified corundum as a component of the chlorite-biotite-cordierite (CBC) alteration zone thought to represent the metamorphosed equivalent of the hydrothermally altered feeder zone for the mineralizing fluids at Izok Lake. Morrison (2004) and Hicken (2012) identified corundum in cordierite-bearing bedrock, whereas Nowak (2012) identified it in the 'moderately altered rhyolite' assemblage.

Intergrowths of corundum were previously identified during visual sorting of gahnite grains recovered from the 250 to 500 µm HMC fraction of till samples from Izok Lake and discrete grains were observed in PTS of one bedrock sample located 2 km northeast of the deposit (Hicken, 2013a). In the previous GSC study (Hicken, 2013a, b), the 250 to 2000 µm HMC fraction of till samples was only examined for the presence of visually distinct blue and red corundum and none were identified in the four till samples used in this study (Hicken et al., 2013b). Thus, it was not considered to be an indicator mineral of the Izok Lake deposit.

The absence of gahnite-corundum intergrowths in the 185 to 250 µm fraction of all but the most proximal (09-MPB-058) sample suggests that corundum and gahnite grains were liberated from one another by crushing and/or abrasion during glacial transport. The presence of grains of intergrown corundum-gahnite in the coarsest (fine sand; 125–185 and 185–250 µm) fractions of till could be an indicator of close proximity (<1 km) to Zn-rich alteration zones. The presence of intergrown grains in the less than 185 µm HMC fractions of till farther down ice is likely the result of these grains having increased resistance to crushing and abrasion as grain size decreases (Dreimanis and Vagners, 1971).

Epidote

The presence of epidote in bedrock PTS and HMC was previously reported by Hicken (2012), Nowak (2012), and Hicken et al. (2013a). Nowak (2012) divided bedrock around the Izok Lake deposit into domains based on the degree of hydrothermal alteration of the protolith, and epidote was reported in metamorphosed bedrock corresponding to least and weakly altered protolith. Epidote grains are coarser (0.2–0.7 mm) in the weakly altered assemblages than in the least altered (0.1–0.3 mm) assemblages. Hicken (2012) reported the presence of epidote grains in four bedrock PTS samples; two samples (diabase dyke and iron formation) collected west of Iznogoudh Lake (>5 km down ice of the Izok Lake deposit), and two samples (schist and gneiss) from metamorphic rocks less than 1.5 km from the Izok Lake deposit. Epidote grains in the two proximal bedrock samples are coarser (0.8–2.0 mm) than those in the two more distal samples (0.2–0.7 mm).

Green epidote grain counts in the 250 to 2000 µm HMC fraction of the four till samples used in this study were visually determined by ODM (GSC, unpub. data, 2019) and are reported in Table 4. In the 250 to 2000 µm HMC fraction, epidote abundance is greatest in down-ice samples (09-MPB-058 and 09-MPB-075), and much lower in the samples located up ice (09-MPB-060) and farthest down ice (12-MPB-902) (GSC, unpub. data, 2019). Epidote abundance in the less than 250 µm HMC fraction is different from the coarser, 250–2000 µm, HMC fraction. Epidote in the less than 250 µm fraction is equally abundant at till sample sites 09-MPB-060 and -075 and less abundant at till sample site 12-MPB-902 (Fig. 9), which suggests that till sample 09-MPB-060 is within the epidote alteration halo of the Izok Lake deposit, or that all of these samples contain a background abundance of metamorphic epidote; however, the location of sample 09-MPB-060 within the calcic alteration zone defined by Morrison (2004) suggest that this sample does contain some hydrothermal-alteration–related epidote. Green epidote has been previously identified as an important indicator of porphyry copper deposits (e.g. Cooke et al., 2014; Plouffe et al., 2016; Plouffe and Ferbey, 2017), where epidote abundance and trace-element composition can be used in tandem to identify hydrothermal carbonate and propylitic alteration halos and assess ore fertility in porphyry copper systems; however, the chemical changes associated with carbonate and propylitic alteration lead to bulk-rock compositions similar to calc-silicate rocks of sedimentary or metasomatic origin (Bonnet and Corriveau, 2007), thus epidote is also common in mineral assemblages that are not associated with hydrothermal activity (Deer et al., 1992). Epidote will need to be identified along with other indicator minerals to serve as a potential vector to VMS mineralization. Future work is needed to investigate the utility of epidote as an indicator mineral for metamorphosed VMS systems, paying careful attention to collecting true regional background samples outside the potentially wide zone of calcic alteration.

Iron oxide minerals

The Fe-oxide minerals hematite, goethite, and magnetite are used as indicator minerals of porphyry copper (e.g. Kelley et al., 2011, Plouffe and Ferbey, 2017) and VMS (e.g. Makvandi et al., 2016; McClenaghan et al., 2017a) mineralization. These minerals can be derived from fresh bedrock, sulfide gossans that were glacially eroded and incorporated into glacial sediments, or postglacial weathering of sulfide grains in till. Automated mineralogical platforms such as MLA cannot distinguish the valence state of individual elements, which makes it difficult to distinguish between Fe-oxide minerals (goethite, limonite, hematite, and magnetite; Sandmann, 2015). The MLA mineral reference library for this project has one entry for an Fe-oxide mineral and although it is possible to further differentiate minerals using

the data gathered by the MLA based on the amplitude of individual elemental peaks, this would have required more time than was available during our routine MLA analysis.

The increase in Fe-oxide mineral abundance in till down ice of the Izok Lake deposit likely represents the incorporation of iron formation, the incorporation of weathered gossanous material from the Izok Lake deposit, the weathering of sulfide grains within till following deposition, or some combination of the three. Mineralized iron-formation makes up a portion of the hanging wall immediately east of the deposit (Morrison, 2004). Iron oxide mineral abundance in the 185 to 250 µm fraction increases in the till progressively farther down ice of sample 09-MPB-058, with the highest value (72.16 normalized grains per 1000 grains) observed in the 185 to 250 µm fraction of till sample 12-MPB-902, located 8 km down ice of mineralization. It is typical for indicator-mineral abundance in till dispersal trains to peak farther down ice, as opposed to immediately down ice, of a bedrock source because source material is progressively incorporated into the dispersal train relative to the reduction in the amount of material transported from up ice from the bedrock source (DiLabio, 1990); this likely accounts for the lower abundance of Fe-oxide minerals identified in till sample 09-MPB-058 (0.5 km down ice) compared to till sample 09-MPB-075 (3 km down ice). The further increase in Fe-oxide mineral abundance in distal till sample 12-MPB-902 may reflect an influx of debris from the WIZ showing, located 2.5 km up ice.

Sulfide ore minerals

The instability of sulfide minerals in oxidizing surface environments, combined with their low resistance to physical abrasion and crushing, results in poor preservation of sulfide minerals in till at surface (Averill, 2001). Of the four Izok Lake samples we studied, chalcopyrite, pyrite, and sphalerite were only detected in the 250 to 2000 µm fraction of till sample 09-MPB-058, immediately down ice of mineralization (Hicken et al., 2013b). Galena was not identified in the 250 to 2000 µm HMC fraction of any of the four samples (Hicken et al., 2013b).

We identified several sulfide minerals in the less than 250 µm HMC fraction of our samples, including chalcopyrite, galena, pyrite, sphalerite, and pyrrhotite. Sample 09-MPB-058, immediately down ice of mineralization, has the highest abundances of all sulfide minerals investigated, with values that could be expected for metal-rich surface till proximal to a VMS deposit in permafrost terrain. This sample contains the only significant abundance of sphalerite identified in this study. The relative abundances of sulfide minerals in the less than 250 µm HMC fraction of this metal-rich sample are sphalerite>pyrite>pyrrhotite>chalcopyrite>galena; this pattern reflects the ranked order of ore elements in the deposit: Zn>Cu>Pb.

Sphalerite was only visually observed in the 250 to 2000 µm HMC fraction of 2 of 53 till samples in the earlier GSC study, 09-MPB-058 and 09-MPB-052, both of which are located down ice of mineralization between Izok Lake and Iznogoudh Lake (Hicken et al., 2013b). Our study detected sphalerite as discrete grains that can contain inclusions of chalcopyrite or pyrite. The low sphalerite abundance in till in all four size fractions is likely the result of some combination of rapid physical abrasion during glacial transport due to low hardness (3.5–4), postglacial chemical weathering, and possible limited direct exposure of sphalerite-bearing zones of the deposit to glacial erosion.

Pyrite is common in mineralized and unmineralized rocks, so it is less useful than chalcopyrite as an indicator mineral of sulfide mineralization. Hicken et al. (2013b) recovered 250 to 2000 µm pyrite in five till samples: 09-MPB-058, -016, -081, -052, and -030, with the highest abundance in sample 09-MPB-081 (56 grains), immediately up ice of mineralization; and 09-MPB-058 (338 grains) and -016 (82 grains), 500 m down ice of mineralization (all grain counts normalized to 10 kg bulk sample weight). Lower abundances were recovered from samples 09-MPB-052 (24 grains) and -030 (13 grains), 1 km and 5 km down ice of mineralization, respectively, and no pyrite grains were recovered from up-ice till sample 09-MPB-060 Hicken et al. (2013b).

Pyrite abundance in the less than 250 µm HMC fraction at Izok Lake differs from the 250 to 2000 µm fraction. Abundance is highest immediately down ice of mineralization but reaches background levels (0.2–0.4 normalized grains per 1000 grains, defined by abundance in up-ice sample 09-MPB-060) in most size fractions at sample site 09-MPB-075, 2.5 km down ice of mineralization (Fig. 10). In the less than 64 µm fraction, pyrite values remain elevated above background (0.06 normalized grains per 1000 grains) at sample site 12-MPB-902, 10 km down ice of mineralization. This suggests that sample site 09-MPB-060 (1 km up ice) may not represent background for most size fractions, or that pyrite in the coarse fraction was rapidly comminuted to the finer fraction by abrasion and crushing during glacial transport. The high abundances of pyrite overlying and just down ice of base-metal mineralization indicate that it can be a useful indicator in combination with other sulfide minerals, and the dispersal distance may be greater when examining the less than 64 µm fraction.

In our study, chalcopyrite is present in the less than 250 µm HMC fraction of the three till samples down ice of mineralization. A small number of grains are also present in the less than 64 µm fraction of sample 09-MPB-060, directly up ice of the deposit (Fig. 10). The presence of chalcopyrite in the less than 250 µm fraction of till is significant because it represents an increase in the dispersal distance down ice: from 1 km for the 250 to 2000 µm HMC fraction to at least 8 km for the less than 250 µm HMC fraction. Chalcopyrite may also have been contributed to the glacial dispersal train from the WIZ showing (Oviatt, 2010).

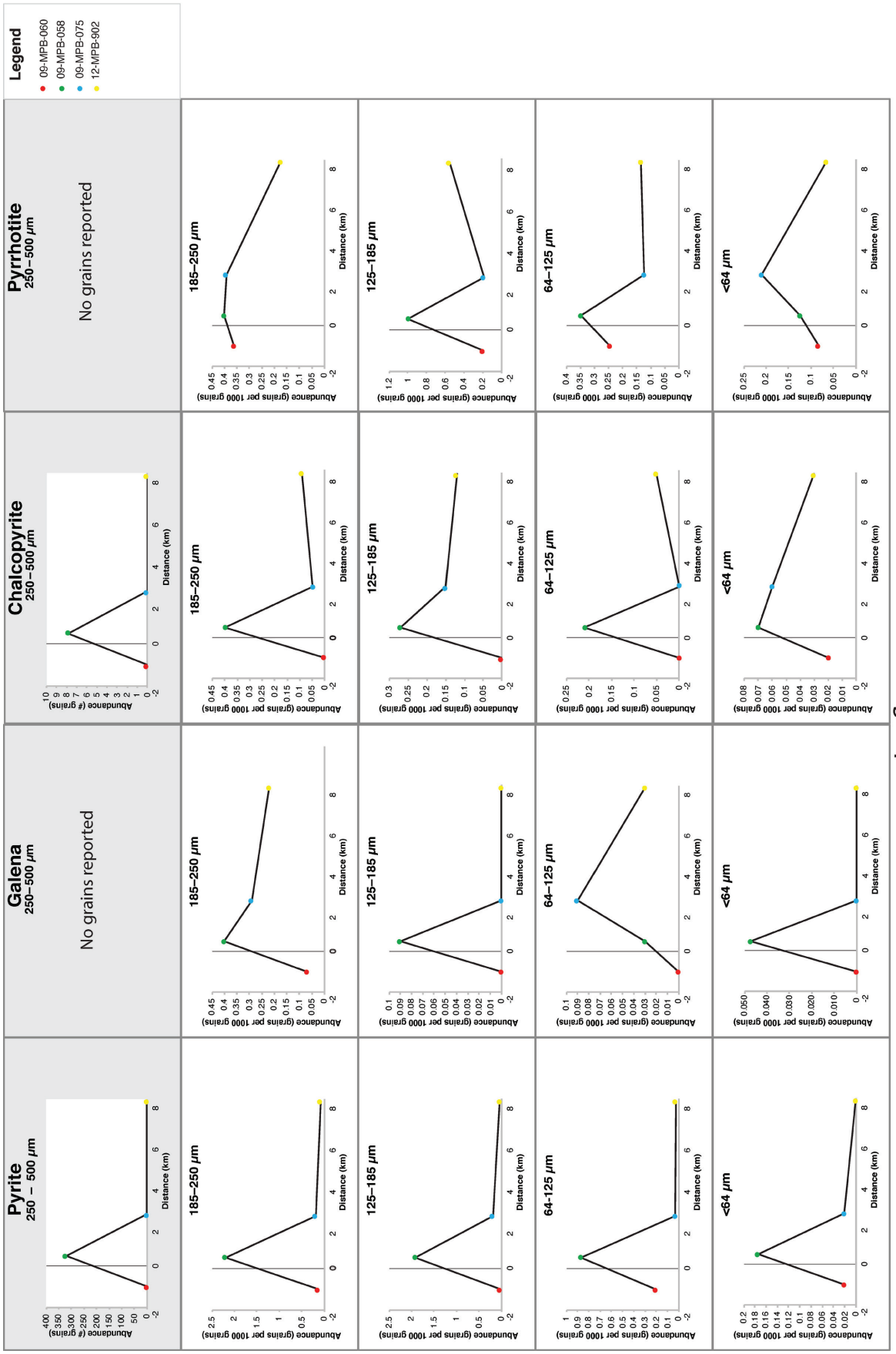

Figure 10. Sulfide grain abundance in the 250–500 µm heavy-mineral concentration (HMC) fraction (visual counts; Hicken et al., 2013b) and the 185 to 250, 125 to 185, 64 to 125, and less than 64 µm HMC fractions (mineral-liberation analysis; this study) of till samples from the Izok Lake deposit, Nunavut. Glacial transport distance is indicated by the black arrow, and the location of mineralization is indicated by a vertical grey line. Sample order, from up ice to distal down ice, is: 09-MPB-060 (1 km up ice), 09-MPB-058 (0.5 km down ice), 09-MPB-075 (2.5 km down ice), and 12-MPB-902 (8 km down ice).

Hicken et al. (2013b) reported the presence of galena in the 250 to 500 µm HMC fraction of only one till sample, collected 1 km down ice of mineralization. Area per cent measurements found minor amounts of galena in the less than 250 µm samples located down ice of the deposit, but the abundance is anomalously high in the 185 to 250 µm fraction of each sample (Table 3). Galena occurs as small inclusions (10–15 µm) within other minerals (garnet, calcic amphibole, and chlorite) in the 185 to 250 µm fraction of samples located up to 8 km down ice. Galena is not identified in the less than 64 µm fraction of the four till samples. This distribution represents a significant increase in galena dispersal distance based on our analysis, from 1 km down ice based on the 250 to 500 µm HMC fraction compared to 8 km down ice based on the less than 250 µm HMC fraction (Fig. 10).

No pyrrhotite was recovered from the coarse, nonferromagnetic HMC of till samples in the previous GSC study because discrete pyrrhotite grains are removed during ferromagnetic separation. Pyrrhotite detected in the less than 250 µm, nonferromagnetic HMC fraction in this study is present as inclusions in composite grains, where the pyrrhotite content is so minor that the magnetic forces of attraction applied during processing could not overcome the mass of the grain. The abundance of pyrrhotite in the less than 250 µm HMC fraction of sample 09-MPB-060, 1 km up ice of mineralization, is comparable to the amount identified in till sample 09-MPB-075, 2.5 km down ice (west) of mineralization (Fig. 10). This distribution suggests that either the abundance of pyrrhotite in till is diminished to regional background levels within 2.5 km down ice, or up-ice sample 09-MPB-060 does not represent regional background for pyrrhotite.

Sisson

Scheelite

Coarse (250–2000 µm) scheelite was previously reported in local till and stream sediments by McClenaghan et al. (2014b, 2017b). In these previous studies, scheelite is most abundant in sample 11-MPB-505, overlying the Ellipse ore zone, and decreased in abundance in sample 11-MPB-567, -525, and -539. No scheelite was recovered from the 250 to 2000 µm fraction of up-ice till sample 11-MPB-520. Scheelite abundance in the less than 250 µm HMC fraction determined using MLA is similar to that reported in the 250 to 2000 µm fraction (Fig. 11). Till samples from farther down ice are needed to discern if there is any difference in the maximum glacial transport distance of scheelite grains in the less than 250 and 250 to 2000 µm fractions.

Wolframite

Coarse (250–2000 µm) wolframite was identified only in a single till sample overlying the deposit; that sample was not examined in this study (McClenaghan et al., 2013a, 2014b, 2015b, 2017b). Wolframite is typically difficult to identify visually because it is similar in appearance to other minerals. Our documentation of wolframite in the less than 250 µm HMC fraction of till down ice of the Sisson deposit (Fig. 11) is likely because MLA identified wolframite chemically using EDS and detected wolframite inclusions in other minerals. Our detection of wolframite in the less than 250 µm HMC fraction of till up to 10 km down ice represents a significant improvement over the visual examination results based on the 250 to 2000 µm HMC fraction; we have delineated a longer dispersal train of wolframite and thus a larger wolframite exploration target.

Molybdenite

Molybdenite was previously identified in the 250 to 2000 µm HMC fraction of till and stream-sediment samples around the Sisson deposit by McClenaghan et al. (2013a, 2014b, 2015b, 2017b). Of the samples examined in that study, only sample 11-MPB-567 contained molybdenite in the 250 to 2000 µm fraction: 87 grains per 10 kg in the 250 to 500 µm and 49 grains per 10 kg in the 500 to 2000 µm fraction (McClenaghan et al. 2013a, 2014b, 2015b, 2017b). The high grain counts in the 250 to 2000 µm fraction correlate with the high molybdenite abundances measured in our study (Table 6). We only identified molybdenite in the less than 250 µm fine fraction of till samples that overlie mineralization, which suggests that molybdenite is fine grained in the deposit and/or was rapidly comminuted to the less than 250 µm fraction during glacial entrainment due to its low hardness (1).

Bismuth minerals

The bismuth minerals joseite (Bi_4TeS_2), native bismuth, bismutite ($(BiO)_2CO_3$), and bismuthinite (Bi2S3) were previously identified in the 250 to 2000 µm fraction of till and stream-sediment samples around the Sisson deposit (McClenaghan et al., 2013a, 2014b, 2017b). Of the five till samples examined in this study, only sample 11-MPB-567 contains coarse bismuth minerals (2 grains bismuthinite per 10 kg till).

The mineral reference library used to classify MLA data in this study does not contain spectra for the individual bismuth mineral species identified by McClenaghan et al. (2017b). Bismuth-bearing minerals were identified in our samples using a mineral spectrum for native Bi (Table 6), but these grains appear to contain other elements. During future work, Bi-bearing minerals will be examined with targeted EPMA to identify their composition and their spectra will be added to the MLA reference library.

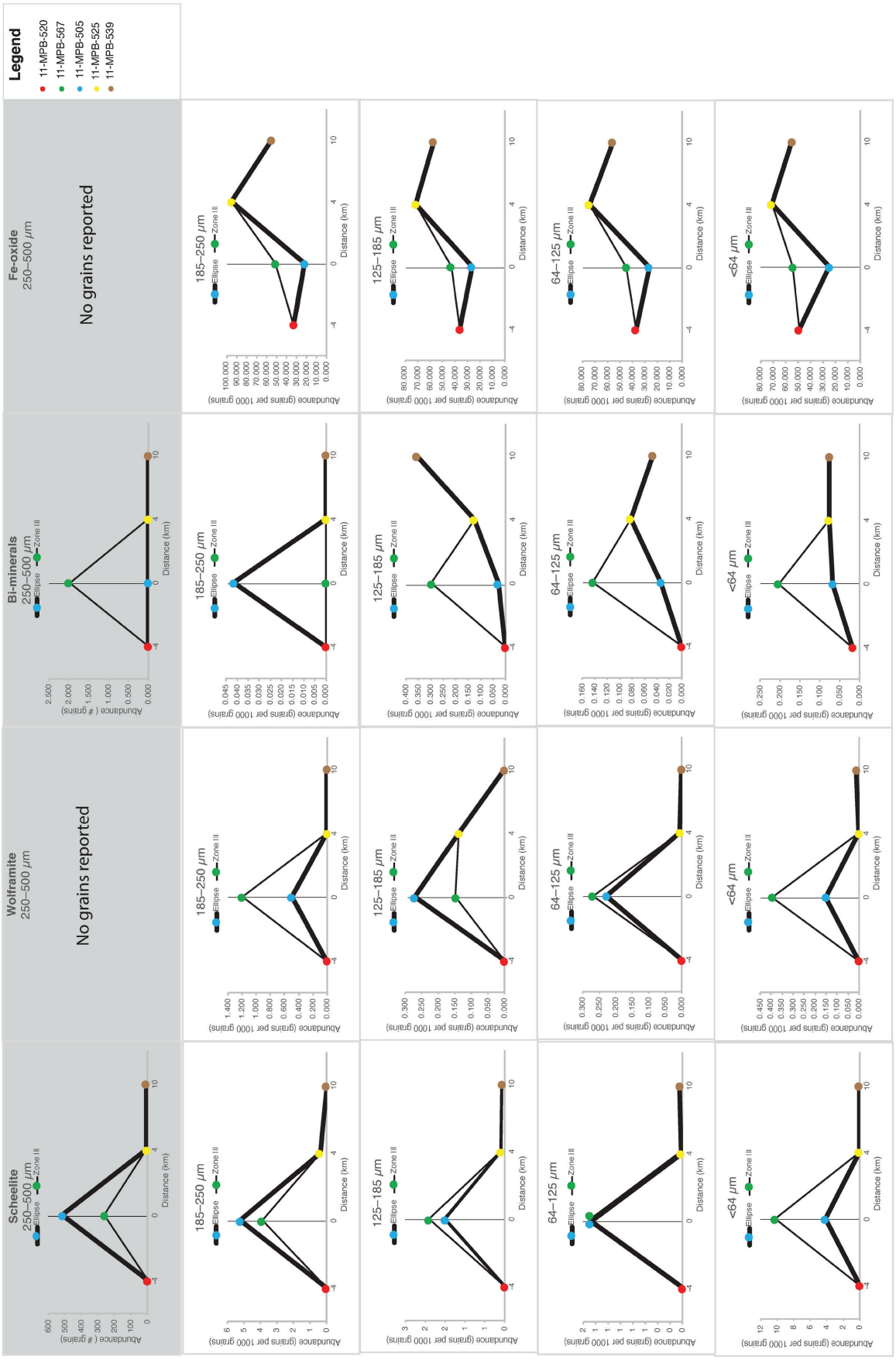

Figure 11. Grain abundance (normalized to grains per 1000 grains) of key ore and alteration indicator minerals in the 185 to 250, 125 to 185, 64 to 125, and less than 64 μm heavy-mineral concentrate (HMC) fractions (mineral-liberation analysis; this study) of five samples from the Sisson deposit, New Brunswick. The x-axis of each is a scaled representation in the direction of ice flow (black arrow). The location of mineralization is denoted by a grey line, and two trendlines depict the inferred decay in indicator mineral abundance along the dispersal train extending from the deposit, taking into account the two separate paths across mineralization (samples 11-MPB-505 and 11-MPB-567).

Iron oxide minerals

The abundance of Fe-oxide minerals is greatest 4 km down ice from mineralization at Sisson in all less than 250 µm fractions (Fig. 11). This distribution pattern does not allow us to directly link Fe-oxide minerals in till to mineralization. Potential relationships between mineralization and Fe-oxide minerals in till will require targeted chemical analysis (i.e. EPMA, LA-ICP-MS).

Other sulfide minerals

Chalcopyrite, arsenopyrite, sphalerite, pyrite, and galena were all identified in the 250 to 2000 µm HMC fraction of till and stream-sediment samples around the Sisson deposit by McClenaghan et al. (2013a, 2014b, 2015b, 2017b); however, only chalcopyrite and pyrite were identified in the 250 to 2000 µm HMC fraction of till samples examined in this study. The 250 to 500 µm fraction of till in sample 11-MPB-567, overlying zone III mineralization, contained 8 grains/10 kg of chalcopyrite and 217 grains/10 kg of pyrite (McClenaghan et al. 2013a, 2014b, 2015b, 2017b).

We identified sulfide minerals in greater abundance in the less than 250 µm fraction of till down ice of the Sisson deposit (Fig. 12), including chalcopyrite, arsenopyrite, galena, and pyrite in sample 11-MPB-539, located 10 km down ice. The presence of fine-grained sulfide minerals in till sample 11-MPB-539 combined with the presence of scheelite in the same sample suggests that these sulfide minerals are likely derived from the Sisson deposit. The presence of these minerals 10 km down ice represents a significant increase in the extent of sulfide mineral dispersal down ice compared to the interpretation based on the 250 to 2000 µm HMC fraction (McClenaghan et al. 2013a, 2014b, 2015b, 2017b). Of particular note is the identification of discrete grains of galena in the 185 to 250 µm fraction of till sample 11-MPB-539. Galena was not identified in the visually inspected 250 to 2000 µm fraction any of the five samples examined in this study (McClenaghan et al. 2013a, 2014b, 2015b, 2017b).

Comparison of sulfide mineral abundance in till at the two test sites

Given that the Izok Lake deposit is a VMS deposit and the minor sulfide minerals at Sisson are predominantly vein hosted, it could be expected that the relative abundance of sulfide mineral grains in till from Izok Lake would be higher than in till from Sisson. Species identified in the less than 250 µm HMC fractions of till from Izok Lake include sphalerite, galena, chalcopyrite, pyrite, and pyrrhotite. At Sisson, a broader range of sulfide minerals were identified in the till, including molybdenite, sphalerite, galena, chalcopyrite, pyrite, and bismuth minerals. Sphalerite and galena are more abundant at Izok Lake (Table 5) whereas chalcopyrite and pyrite are more abundant at Sisson (Table 7).

The differences in the presence and abundance of sulfide mineral species in till overlying Izok Lake and Sisson mineralization are a function of the nature of the mineralization, the proximity of the till sample to mineralization, the grade of mineralization that subcropped and was exposed to glacial erosion, the areal extent of the subcropping mineralization, the till thickness, the preglacial weathering of bedrock and postglacial weathering of till, and complexity of ice flow directions.

At Izok Lake, the gahnite dispersal train is a palimpsest pattern (Fig. 2) produced by two ice flow events to the southwest and northwest of the deposit (Paulen et al., 2013). Although the Sisson region has also undergone several glacial events, the dispersal train has been shaped predominantly by southeast ice flow (Fig. 3) during the Early Wisconsinan (with some possible minor reworking in the Middle to Late Wisconsinan; Seaman et al., 2007). The indicator minerals in till down ice of the Izok Lake deposit have been spread over a greater area than at Sisson, which likely reduced the relative abundances of indicator minerals in till at Izok Lake.

The three subcropping massive-sulfide lenses at Izok Lake extend over an area of approximately 0.4 × 0.8 km, whereas the vein-hosted mineralization at Sisson subcrops over a larger (1 × 2 km) area (Rennie et al., 2013). This difference in the areal extent of metal-rich subcropping surface exposed to glacial erosion likely influenced the overall abundance of metal-rich debris in till down ice of the deposits. Till samples from Izok Lake were collected from frost boils in permafrost terrain (Shilts, 1978; Hicken et al., 2012, 2013b), whereas samples from Sisson were collected from the unoxidized till in freshly dug trenches, road cuts, and hand-dug holes in boreal forest (non-permafrost) terrain. This difference in sampling media may also have impacted the preservation and/or representation of sulfide minerals in the resultant till HMC.

Preferred grain size for MLA

Wilton and Winter (2012) and Wilton et al. (2017) suggested that the 125 to 185 µm HMC fraction of till is the most suitable for MLA, based on the number of indicator mineral grains detected and the MLA processing time compared to grain mounts of less than 125 µm fractions; however, the results from Izok Lake and Sisson suggest that there is valuable information in the 185 to 250 µm fraction, particularly regarding the abundance of sulfide mineral inclusions. At both sites, sulfide mineral (chalcopyrite, galena, sphalerite, and pyrite) inclusions are most abundant in the 185 to 250 µm fraction, followed by the 125 to 185 µm fraction. Three other key indicator minerals (gahnite at Izok Lake, scheelite and wolframite at Sisson) are also most abundant in these size fractions.

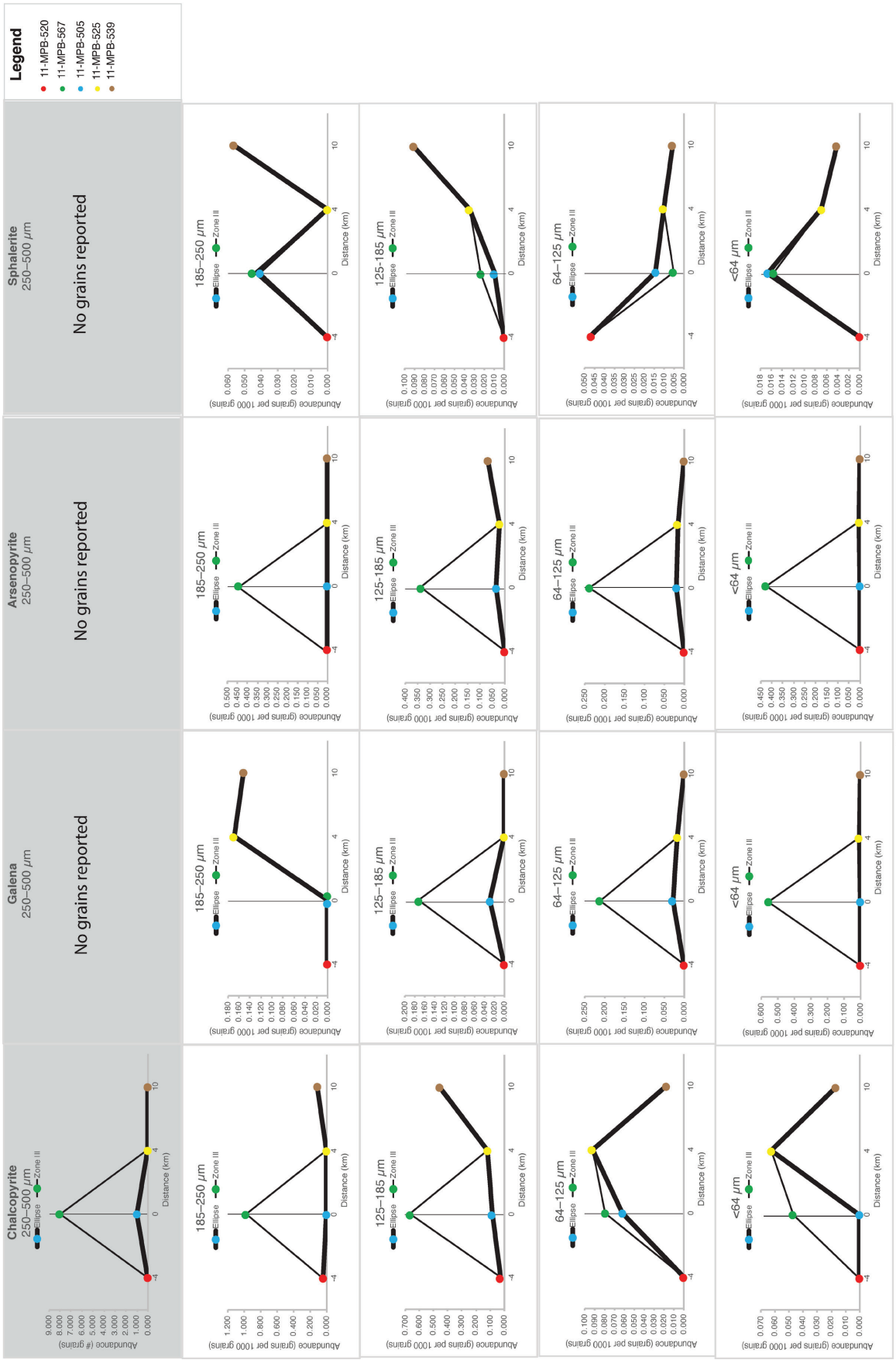

Figure 12. Grain abundance (normalized to grains per 1000 grains) of key sulfide indicator minerals in the 185 to 250, 125 to 185, 64 to 125, and less than 64 μm heavy-mineral concentrate (HMC) fractions (mineral-liberation analysis; this study) of five samples from the Sisson deposit, New Brunswick. The x-axis of each is a scaled representation in the direction of ice flow (black arrow). The location of mineralization is denoted by a grey line, and two trendlines depict the inferred decay in indicator mineral abundance along the dispersal train extending from the deposit, taking into account the two separate paths across mineralization (samples 11-MPB-505 and 11-MPB-567).

Based on our results, the 125 to 250 µm fraction of till HMC is the optimal fraction for MLA of indicator minerals in till to identify targets for sulfide-bearing deposit exploration. Mounting the 125 to 250 µm grains as one fraction, instead of separating it into two (125–185 and 185–250 µm) fractions, has the advantage of higher indicator and overall grain counts, which improves statistical robustness; and the ability to identify intergrown minerals such as corundum and gahnite, which might become separated in finer fractions, as discussed. The 185 to 250 and 125 to 185 µm fractions combined represent the fine sand fraction of the Wentworth grain-size scale (Wentworth, 1922).

The abundances of indicator minerals in the less than 250 µm fractions is greater than those reported by visual picking of the coarse 250 to 2000 µm HMC fraction of the same samples. Many indicator mineral grains that were identified, especially the sulfide minerals, occur as inclusions within grains of other minerals rather than as discrete grains, and were detected in this study because polished epoxy grain mounts were analyzed; inclusions cannot be easily identified by visual examination of whole grains, thus they were not identified in studies of the 250 to 2000 µm fraction.

CONCLUSIONS

This study is the first examination of the less than 250 µm HMC fraction of till samples from around a high metamorphic grade (upper amphibolite–sillimanite) VMS deposit in permafrost terrain and a sub-greenschist granite-hosted W-Mo deposit using automated mineralogical techniques. Data reported here can be compared to future automated mineralogy studies of the fine fraction of till to establish background and anomalous abundances that could be expected in till close to such deposit types. Major findings of our study include the following:

1. Common ore (chalcopyrite, galena, pyrite, sphalerite, and pyrrhotite) and associated alteration (gahnite, corundum, epidote, Fe-oxide, and staurolite) minerals of metamorphosed VMS deposits are detected in the fine (<250 µm) HMC fraction of till from the Izok Lake area. The less than 250 µm HMC from Sisson contains ore minerals (scheelite, wolframite, and molybdenite), sulfide minerals (chalcopyrite, arsenopyrite, sphalerite, pyrite, galena, and pentlandite), and associated minerals (bismuth minerals, Fe-oxide minerals).

2. Anomalous abundances of sulfide minerals in the less than 250 µm HMC fraction extend farther in till down ice of the Izok Lake and Sisson deposits than has been previously recorded from discrete grains in the visually sorted 250 to 2000 µm fraction. At Izok Lake, chalcopyrite and galena were detected up to 8 km down ice, a significant increase from the 1.3 km down-ice dispersal distance reported for these minerals in the 250 to 2000 µm HMC fraction (Hicken et al., 2013b; McClenaghan et al., 2015a). Chalcopyrite, arsenopyrite, pyrite, and galena were detected in till 10 km down ice of the Sisson deposit, where previously they had only been identified in till samples overlying mineralization (McClenaghan et al. 2013a, 2014b, 2015b, 2017b).

3. It is time consuming to manually sort and visually identify indicator minerals in the hundreds or thousands of grains in the 250 to 2000 µm HMC fraction of till. Automated mineralogical analysis of the less than 250 µm HMC fraction makes quantifying the abundance of all minerals straightforward and precise, once the grains have been sieved into smaller size fractions and mounted. Round mounts of less than 250 µm till HMC fractions present 50 000 to 300 000 grains for analysis, many times more than are examined in 250 to 2000 µm material.

4. Future research should investigate the use of trace-element compositional analysis of all indicator minerals identified in the less than 250 µm HMC fraction using automated methods because many recent bedrock studies on trace elements in alteration/metamorphic minerals have been focused on increasing deposit exploration footprints. The grain maps generated by MLA serve as guides for more sensitive mineral chemistry tools such as EPMA or LA-ICP-MS.

5. Automated mineralogy can identify indicator minerals that are difficult or impossible to distinguish using traditional visual analysis of the coarser fraction; present only as small inclusions (e.g. sulfide minerals, especially galena) in larger grains of other minerals; and/or indicative of mineralization where intergrown or interlocked with specific other minerals (e.g. corundum and gahnite). Conversely, the colour of grains recorded during visual analysis methods can be used to rapidly distinguish minor-element enrichment in some minerals (e.g. red for Mn-epidote or Cr-rich rutile). Mineral-liberation analysis can only recognize these grains if corresponding X-ray spectra have already been identified and added to the mineral reference library. Visual and automated methods can be applied in tandem following density concentration to provide rapid and inexpensive evaluation of bulk abundances of indicator mineral grains (visual sorting) and follow-up automated analysis of polished samples to identify distinct minerals and mineral inclusions (particularly sulfides) that cannot be detected visually. Mineral association, liberation, and morphological data can be collected at the same time.

6. Use of the 125 to 250 µm (fine-sand) HMC fraction of till will reduce the scanning time necessary for each sample compared to finer fractions, while still presenting 50 000 to 100 000 grains for analysis on a polished grain mount surface. For the two deposit types examined in this study, the fine-sand (125–250 µm) fraction of till HMC is the most effective fraction to use with automated mineralogy for detection of indicator mineral anomalies.

7. Reporting indicator mineral abundance as a normalized grain count and area per cent allows for inferences about mineral occurrence that would not be possible using only one metric. Normalization of grain count values to 1000 grains ensures that abundance data are intuitive and can be compared between samples and projects. The combination of grain count data sets with area per cent values can suggest whether a mineral is present as smaller numbers of larger grains or many small grains.
8. The methods developed and demonstrated are optimal for investigations of indicator minerals in the less than 250 µm HMC fraction of till samples that have already been analyzed using other methods (visual sorting, matrix geochemistry) and that display interesting matrix (<63 µm) geochemistry and/or indicator mineral signatures in the greater than 250 µm HMC fraction.

FUTURE RESEARCH

The establishment of accurate background indicator mineral abundance is crucial to the success of any till indicator mineral exploration program. Initial till sampling programs should analyze samples from a widely spaced grid based on knowledge of regional bedrock geology and ice-flow history. Detailed follow-up till sampling of areas of interest should include samples taken up ice of any identified anomalies because samples collected within the alteration halo of mineralization will not reflect background levels for some indicator minerals.

We continue with our interpretation of data from the Sisson deposit, with targeted EPMA of several minerals of interest planned to refine the MLA mineral reference library and identify unknown grains in the till samples. The chemical composition of bismuth minerals, among others, will be evaluated. The last phase of our project will investigate the less than 250 µm HMC fraction of till from the Triple B kimberlite, in the Lake Timiskaming kimberlite field, Ontario, to characterize the fine-grained mineralogy of down-ice till.

ACKNOWLEDGMENTS

Support for this project was provided by Natural Resources Canada's Targeted Geoscience Initiative Program (TGI-5) through a direct funding of analysis and Research Affiliate Program (RAP) bursary to the senior author as part of his Ph.D. research. We thank the team at Overburden Drilling Management Limited for their assistance with all questions relating to sample processing and indicator mineral methods, and Agatha Dobosz and Brian Joy at Queen's University for instruction on the operation of the microanalytical instruments used in the study. We thank Stuart Averill (ODM) and Alain Plouffe (GSC) for reviews of the manuscript. We thank Jan Peter (GSC) for general discussions about the geology of VMS deposits and editorial handling.

REFERENCES

Averill, S.A., 2001. The application of heavy indicator mineralogy in mineral exploration; *in* Drift exploration in glaciated terrain, (ed.) M.B. McClenaghan, P.T. Bobrowsky, G.E.M. Hall, and S. Cook; Geological Society of London, Special Publication, no. 185, p. 69–81. https://doi.org/10.1144/Gsl.Sp.2001.185.01.04.

Averill, S.A., 2011. Viable indicator minerals in surficial sediments for two major base metal deposit types: Ni-Cu-PGE and porphyry Cu; Geochemistry: Exploration, Environment, Analysis, v. 11, no. 4, p. 279–291. https://doi.org/10.1144/1467-7873/10-IM-022

Averill, S.A., 2013. Discovery and delineation of the Rainy River gold deposit using glacially dispersed gold grains sampled by deep overburden drilling: a 20-year odyssey; *in* New frontiers for exploration in glaciated terrain, (ed.) R. Paulen and M.B. McClenaghan; Geological Survey of Canada, Open File 7374, p. 37–46. https://doi.org/10.4095/300290

Averill, S.A., 2017. The Blackwater gold-spessartine-pyrolusite dispersal trains, British Columbia, Canada: influence of sampling depth on indicator mineralogy and geochemistry; Geochemistry: Exploration, Environment, Analysis, v. 17, no. 1, p. 43–60. https://doi.org/10.1144/geochem2015-399

Averill, S.A. and Huneault, R.G., 2016. Basic indicator mineral math: why visual analysis of the entire heavy mineral fraction of large sediment samples is required on indicator mineral exploration programs in glaciated terrains; EXPLORE, v. 172, p. 1–14.

Averill, S.A. and Zimmerman, J.R., 1986. The riddle resolved: the discovery of the Partridge gold zone using sonic drilling in glacial overburden at Waddy Lake, Saskatchewan; Canadian Geology Journal of the Canadian Institute of Mining and Metallurgy, v. 1, p. 14–20.

Blaskovich, R.J., 2013. Characterizing waste rock using automated quantitative electron microscopy; M.Sc. thesis, The University of British Columbia, Vancouver, British Columbia, 310 p.

Bleeker, W. and Hall, B., 2007. The Slave Craton: geological and metallogenic evolution; *in* Mineral deposits of Canada: a synthesis of major deposit types, district metallogeny, the evolution of geological provinces, and exploration methods, (ed.) W.D. Goodfellow; Geological Association of Canada, Mineral Deposits Division, Special Publication No. 5, p. 849–879.

Bleeker, W., Ketchum, J.W., Jackson, V.A., and Villeneuve, M.E., 1999. The Central Slave basement complex, Part I: its structural topology and autochthonous cover; Canadian Journal of Earth Sciences, v. 36, p. 1083–1109. https://doi.org/10.1139/e98-102

Bonnet, A. and Corriveau, L., 2007. Alteration vectors to metamorphosed hydrothermal systems in gneissic terranes; *in* Mineral deposits of Canada: a synthesis of major deposit types, district metallogeny, the evolution of geological provinces, and exploration methods, (ed.) W.D. Goodfellow; Geological Association of Canada, Mineral Deposits Division, Special Publication No. 5, p. 1035–1049.

Buchan, K.L. and Ernst, R., 2004. Diabase dyke swarms and related units in Canada and adjacent regions; Geological Survey of Canada, Open File 7464, 1 map. https://doi.org/10.4095/293149

Cooke, D., Baker, M., Hollings, P., Sweet, G., Chang, Z., Danyushevsky, L., Gilbert, S., Zhou, T., White, N., Gemmel, J., and Inglis, S., 2014. New advances in detecting the distal geochemical footprints of porphyry systems – epidote mineral chemistry as a tool for vectoring and fertility assessments; *in* Building exploration capability for the 21st century, (ed.) K.D. Kelley and H.C. Golden; Society of Economic Geologists, p. 127–152.

Costello, K., Senkow, M., Bigio, A., Budkewitsch, P., Ham, L., and Mate, D., 2012. Nunavut mineral exploration, mining and geoscience overview 2011; Aboriginal Affairs and Northern Development Canada, 71 p.

Day, S.J.A., Lariviere, J.M., McNeil, R.J., Friske, P.W.B., Cairns, S.R., McCurdy, M.W., and Wilson, R.S., 2007. Regional stream sediment and water geochemical data, Horn Plateau area, Northwest Territories (parts of NTS 85E, 85F, 85K, 85L, 95H, 95I and 95J) including analytical, mineralogical, and kimberlite indicator mineral data; Geological Survey of Canada, Open File 5478, 1 CD-ROM. https://doi.org/10.4095/224262

Deer, W., Howie, R., and Zussman, J., 1992. An introduction to the rock forming minerals, 2nd ed., England, Longman Scientific and Technical, 696 p.

Dietvorst, E.J., 1981. Biotite breakdown and the formation of gahnite in metapelitic rocks from Kemiö, Southwest Finland; Contributions to Mineralogy and Petrology, v. 75, no. 4, p. 327–337.

DiLabio, R., 1990. Glacial dispersal trains; *in* Glacial indicator tracing, (ed.) R. Kujansuu and M. Saarnisto; A.A. Balkema, Rotterdam, Netherlands, p. 109–122.

Dredge, L.A., Kerr, D.E., and Ward, B.C., 1996a. Surficial geology, Point Lake, District of Mackenzie, Northwest Territories; Geological Survey of Canada, Map 1890A, scale 1:125 000 https://doi.org/10.4095/208591

Dredge, L.A., Ward, B.C., and Kerr, D.E., 1996b. Trace element geochemistry and gold grain results from till samples, Point Lake, Northwest Territories (86H); Geological Survey of Canada, Open File 3317, 163 p. https://doi.org/10.4095/208289

Dredge, L.A., Kerr, D.E., and Wolfe, S.A., 1999. Surficial materials and related ground ice conditions, Slave Province, N.W.T., Canada; Canadian Journal of Earth Sciences, v. 36, no. 7, p. 1227–1238. https://doi.org/10.1139/e98-087

Dreimanis, A. and Vagners, U., 1971. Bimodal distribution of rock and mineral fragments in basal tills; *in* Till, a symposium, (ed.) R.P Goldthwaite; Ohio State University Press, Columbus, Ohio, p. 237–250.

Dyke, A.S., 2004. An outline of North American deglaciation with emphasis on central and northern Canada; *in* Developments in Quaternary Sciences, Elsevier, p. 373–424.

Dyke, A.S. and Prest, V.K., 1987a. Late Wisconsinan and Holocene history of the Laurentide ice sheet; Géographie physique et Quaternaire, v. 41, no. 2, p. 237–263. https://doi.org/10.7202/032681ar

Dyke, A.S. and Prest, V.K., 1987b. Late Wisconsinan and Holocene retreat of the Laurentide ice sheet; Geological Survey of Canada, Map 1702A, scale 1:5 000 000 https://doi.org/10.4095/122842

Falck, H., Day, S., Pierce, K.L., Cairns, S.R., and Watson, D., 2015. Geochemical, mineralogical and indicator mineral data for stream silt sediment, heavy mineral concentrates and waters, Flat River area, Northwest Territories, (part of NTS 95E, 105H and 105I); Northwest Territories Geoscience Office, NWT Open Report 2015-002.

Fyffe, L. and Thorne, K.G. (comp.), 2010. Polymetallic deposits of Sisson Brook and Mount Pleasant, New Brunswick, Canada; New Brunswick Department of Natural Resources, Lands, Minerals and Petroleum Division, Field Guide No. 3, 68 p.

Fyffe, L., Pajari, G., Jr., and Cherry, M., 1981. The Acadian plutonic rocks of New Brunswick; Maritime Sediments and Atlantic Geology, v. 17, p. 23–36.

Fyffe, L., Thorne, K., Dunning, G., and Martin, D., 2008. U-Pb geochronology of the Sisson Brook granite porphyry, York County, west-central New Brunswick; *in* Geological Investigations in New Brunswick for 2007, (ed.) G.L. Martin; New Brunswick Department of Natural Resources, Minerals, Policy, and Planning Division, Mineral Resource Report 2008–1, p. 35–54.

Galley, A.G., Hannington, M.D., and Jonasson, I., 2007. Volcanogenic massive sulphide deposits; *in* Mineral deposits of Canada: a synthesis of major deposit types, district metallogeny, the evolution of geological provinces, and exploration methods, (ed.) W.D. Goodfellow; Geological Association of Canada, Mineral Deposits Division, Special Publication No. 5, p. 141–161.

Ghosh, B. and Praveen, M., 2008. Indicator minerals as guides to base metal sulphide mineralisation in Betul Belt, central India; Journal of Earth System Science, v. 117, p. 521–536. https://doi.org/10.1007/s12040-008-0050-x

Hashmi, S., Ward, B., Plouffe, A., Leybourne, M., and Ferbey, T., 2015. Geochemical and mineralogical dispersal in till from the Mount Polley Cu-Au porphyry deposit, central British Columbia, Canada; Geochemistry: Exploration, Environment, Analysis, v. 15, p. 234–249. https://doi.org/10.1144/geochem2014-310

Hicken, A., 2012. Glacial dispersal of indicator minerals from the Izok Lake Zn-Cu-Pb-Ag VMS deposit, Nunavut, Canada; M.Sc. thesis, Queen's University, Kingston, Ontario, 645 p.

Hicken, A.K., McClenaghan, M.B., Paulen, R.C., and Layton-Matthews, D., 2012. Till geochemical signatures of the Izok Lake Zn-Cu-Pb-Ag volcanogenic massive sulphide deposit; Geological Survey of Canada, Open File 7046, 118 p. https://doi.org/10.4095/292140

Hicken, A.K., McClenaghan, M.B., Layton-Matthews, D., Paulen, R.C., Averill, S.A., and Crabtree, D., 2013a. Indicator mineral signatures of the Izok Lake Zn-Cu-Pb-Ag volcanogenic massive sulphide deposit, Nunavut: Part 1 bedrock samples; Geological Survey of Canada, Open File 7173, 112 p. https://doi.org/10.4095/292210

Hicken, A.K., McClenaghan, M.B., Layton-Matthews, D., Paulen, R.C., Averill, S.A., and Crabtree, D., 2013b. Indicator mineral signatures of the Izok Lake Zn-Cu-Pb-Ag volcanogenic massive sulphide deposit, Nunavut: Part 2 till; Geological Survey of Canada, Open File 7343, 48 p. https://doi.org/10.4095/293033

Hulkki, H., Taivalkoski, A., and Lehtonen, M., 2018. Signatures of Cu (-Au) mineralisation reflected in inorganic and heavy mineral stream sediments at Vähäkurkkio, north-western Finland; Journal of Geochemical Exploration, v. 188, p. 156–171. https://doi.org/10.1016/j.gexplo.2018.01.012

Kelley, K.D., Eppinger, R.G., Lang, J., Smith, S.M., and Fey, D.L., 2011. Porphyry Cu indicator minerals in till as an exploration tool: example from the giant Pebble porphyry Cu-Au-Mo deposit, Alaska, USA; Geochemistry: Exploration, Environment, Analysis, v. 11, p. 321–334. https://doi.org/10.1144/1467-7873/10-IM-041

Kjellsen, K., Monsøy, A., Isachsen, K., and Detwiler, R., 2003. Preparation of flat-polished specimens for SEM-backscattered electron imaging and X-ray microanalysis—importance of epoxy impregnation; Cement and Concrete Research, v. 33, no. 4, p. 611–616. https://doi.org/10.1016/S0008-8846(02)01029-3

Lamothe, M., 1992. Pleistocene stratigraphy and till geochemistry of the Miramichi zone, New Brunswick; Geological Survey of Canada, Bulletin 433, 58 p. https://doi.org/10.4095/183878

Layton-Matthews, D., Hamilton, C., and McClenaghan, M.B., 2014. Mineral chemistry: modern techniques and applications to exploration; *in* Application of indicator mineral methods to mineral exploration, (ed.) M.B. McClenaghan, A. Plouffe, and D. Layton-Matthews; Geological Survey of Canada, Open File 7553, p. 9–18.

Lehtonen, M., Lahaye, Y., O'Brien, H., Lukkari, S., Marmo, J., and Sarala, P., 2015. Novel technologies for indicator mineral-based exploration; Geological Survey of Finland, Special Paper 57, p. 23–62.

Lougheed, H.D., McClenaghan, M.B., and Layton-Matthews, D., 2018. Mineral markers of base metal mineralization: progress report on the identification of indicator minerals in the fine heavy mineral fraction; *in* Targeted Geoscience Initiative: 2017 report of activities, (ed.) N. Rogers; Geological Survey of Canada, Open File 8373, p. 101–108. https://doi.org/10.4095/306605

Lougheed, H.D., McClenaghan, M.B., Layton-Matthews, D., and Leybourne, M.I., 2019. Evaluation of single-use nylon screened sieves for use with fine-grained sediment samples; Geological Survey of Canada, Open File 8613, 13 p. https://doi.org/10.4095/315138

Lougheed, H.D., McClenaghan, M.B., Layton-Matthews, D., and Leybourne, M., 2020. Exploration potential of fine-fraction heavy mineral concentrates from till using automated mineralogy: a case study from the Izok Lake Cu–Zn–Pb–Ag VMS deposit, Nunavut, Canada; Minerals, v. 10, no. 4, p. 310. https://doi.org/10.3390/min10040310

Makvandi, S., Ghasemzadeh-Barvarz, M., Beaudoin, G., Grunsky, E.C., McClenaghan, M.B., and Duchesne, C., 2016. Principal component analysis of magnetite composition from volcanogenic massive sulphide deposits: case studies from the Izok Lake (Nunavut, Canada) and Halfmile Lake (New Brunswick, Canada) deposits; Ore Geology Reviews, v. 72, p. 60–85. https://doi.org/10.1016/j.oregeorev.2015.06.023

McClenaghan, M.B., 2005. Indicator mineral methods in mineral exploration; Geochemistry: Exploration, Environment, Analysis, v. 5, no. 3, p. 233–245. https://doi.org/10.1144/1467-7873/03-066

McClenaghan, M.B., 2011. Overview of common processing methods for recovery of indicator minerals from sediment and bedrock in mineral exploration; Geochemistry: Exploration, Environment, Analysis, v. 11, p. 265–278. https://doi.org/10.1144/1467-7873/10-IM-025

McClenaghan, M.B. and Cabri, L.J., 2011. Review of gold and platinum group element (PGE) indicator minerals methods for surficial sediment sampling; Geochemistry: Exploration, Environment, Analysis, v. 11, no. 4, p. 251–263. https://doi.org/10.1144/1467-7873/10-IM-026

McClenaghan, M.B. and Kjarsgaard, B.A., 2007. Indicator mineral and surficial geochemical exploration methods for kimberlite in glaciated terrain: examples from Canada; *in* Mineral deposits of Canada: a synthesis of major deposit types, district metallogeny, the evolution of geological provinces, and exploration methods, (ed.) W.D. Goodfellow; Geological Association of Canada, Mineral Deposits Division, Special Publication No. 5, p. 983–1006.

McClenaghan, M.B. and Paulen, R.C., 2018. Application of till mineralogy and geochemistry to mineral exploration; Chapter 20 in Past glacial environments (second edition), (ed.) J. Menzies and J. Van der Meer; Elsevier, Amsterdam, Netherlands p. 689–751. https://doi.org/10.1016/B978-0-08-100524-8.00022-1

McClenaghan, M.B., Hicken, A.K., Paulen, R.C., and Layton-Matthews, D., 2012. Indicator mineral counts for regional till samples around the Izok Lake Zn-Cu-Pb-Ag VMS deposit, Nunavut; Geological Survey of Canada, Open File 7029, 13 p. https://doi.org/10.4095/289837

McClenaghan, M.B., Parkhill, M.A., Averill, S.A., Pronk, A.G., Seaman, A.A., Boldon, R., McCurdy, M.W., and Rice, J.M., 2013a. Indicator mineral abundance data for bedrock, till, and stream sediment samples from the Sisson W-Mo deposit, New Brunswick; Geological Survey of Canada, Open File 7387, 18 p. https://doi.org/10.4095/292670

McClenaghan, M.B., Parkhill, M., Seaman, A., Pronk, A., Pyne, M., Rice, J., and Hashmi, S., 2013b. Till geochemical signatures of the Sisson W-Mo deposit, New Brunswick; Geological Survey of Canada, Open File 7430, 53 p. https://doi.org/10.4095/292837

McClenaghan, M.B., Parkhill, M.A., Averill, S.A., and Kjarsgaard, I.M., 2013c. Indicator mineral signatures of the Sisson W-Mo deposit, New Brunswick: part 1 bedrock samples; Geological Survey of Canada, Open File 7431, 29 p. https://doi.org/10.4095/292805

McClenaghan, M.B., Holmes, D.R.S., Averill, S.A., Paulen, R.C., and Layton-Matthews, D., 2014a. Physical features indicating the glacial transport distance of gahnite from the Izok Lake Cu-Zn-Pb-Ag VMS deposit, Nunavut; Geological Survey of Canada, Open File 7603, 15 p. https://doi.org/10.4095/293878

McClenaghan, M.B., Parkhill, M.A., Seaman, A.A., Pronk, A.G., Averill, S., Rice, J.M., and Pyne, M., 2014b. Indicator mineral signatures of the Sisson W-Mo deposit, New Brunswick: Part 2 till; Geological Survey of Canada, Open File 7467, 31 p. https://doi.org/10.4095/293349

McClenaghan, M.B., Paulen, R., Layton-Matthews, D., Hicken, A., and Averill, S., 2015a. Glacial dispersal of gahnite from the Izok Lake Zn-Cu-Pb-Ag VMS deposit, northern Canada; Geochemistry: Exploration, Environment, Analysis, v. 15, no. 4, p. 333–349. https://doi.org/10.1144/geochem2014-317

McClenaghan, M.B., Parkhill, M.A., Pronk, A.G., McCurdy, M.W., Boldon, G.R., Leybourne, M.I., Pyne, R.M., and Rice, J.M., 2015b. Geochemical and indicator mineral data for stream sediments and water around the Sisson W-Mo deposit, New Brunswick, (NTS 21-J/06, 21-J/07); Geological Survey of Canada, Open File 7756, 62 p. https://doi.org/10.1144/geochem2011-083

McClenaghan, M.B., Parkhill, M.A., Pronk, A.G., Seaman, A.A., McCurdy, M.W., Poulin, R.S., McDonald, A.M., Kontak, D.J., and Leybourne, M.I., 2015c. Till, stream sediment, and stream water geochemical signatures of intrusion-hosted Sn-W deposits; examples from the Sisson W-Mo and Mount Pleasant Sn-W-Mo-Bi-In deposits, New Brunswick; *in* TGI-4 intrusion related mineralisation project: new vectors to buried porphyry-style mineralisation, (ed.) N. Rogers; Geological Survey of Canada, Open File 7843, p. 39–58. https://doi.org/10.4095/296465

McClenaghan, M.B., Budulan, G., Parkhill, M.A., Layton-Matthews, D., and Crabtree, D., 2017a. Indicator mineral signatures of the Halfmile Lake Zn-Pb-Cu volcanogenic massive sulphide deposit, Bathurst, New Brunswick: Part 2 – till data; Geological Survey of Canada, Open File 8111, 38 p. https://doi.org/10.4095/299554

McClenaghan, M.B., Parkhill, M., Pronk, A., Seaman, A., McCurdy, M., and Leybourne, M., 2017b. Indicator mineral and geochemical signatures associated with the Sisson W–Mo deposit, New Brunswick, Canada; Geochemistry: Exploration, Environment, Analysis, v. 17, no. 4, p. 297–313. https://doi.org/10.1144/geochem2015-396

McClenaghan, M.B., Paulen, R.C., and Oviatt, N.M., 2018. Geometry of indicator mineral and till geochemistry dispersal fans from the Pine Point Mississippi Valley-type Pb-Zn district, Northwest Territories, Canada; Journal of Geochemical Exploration, v. 190, p. 69–86.

Money, P. and Heslop, J., 1976. Geology of the Izok Lake massive sulphide deposit; Canadian Mining Journal, v. 97, no. 5, p. 24–27.

Morrison, I.R., 2004. Geology of the Izok massive sulphide deposit, Nunavut territory, Canada; Exploration and Mining Geology, v. 13, no. 1–4, p. 25–36. https://doi.org/10.2113/gsemg.13.1-4.25

Morrison, I. and Balint, F., 1993. Geology of the Izok Lake massive sulphide deposits, Northwest Territories, Canada; *in* World Zinc'93: proceedings of the international symposium on zinc, 10–13 October 1993, Hobart, Tasmania, (ed.) I.G. Matthew; The Australasian Institute of Mining and Metallurgy, Parkville, Victoria, p. 161–170.

Nast, H.J. and Williams-Jones, A.E., 1991. The role of water-rock interaction and fluid evolution in forming the porphyry-related Sisson Brook W-Cu-Mo deposit, New Brunswick; Economic Geology, v. 86, no. 2, p. 302–317. https://doi.org/10.2113/gsecongeo.86.2.302

Nowak, R., 2012. The nature and significance of high-grade metamorphism and intense deformation in the Izok VHMS alteration halo and deposit; M.Sc. thesis, Colorado School of Mines, Golden, Colorado, 194 p.

Oviatt, N.M. 2010. Till geochemistry of the West Iznogoudh Zn showing, Point Lake map sheet (86H), Nunavut; B.Sc. thesis, University of Calgary, Calgary, Alberta.

Paulen, R.C., McClenaghan, M.B., and Hicken, A.K., 2013. Regional and local ice-flow history in the vicinity of the Izok Lake Zn-Cu-Pb-Ag deposit, Nunavut; Canadian Journal of Earth Sciences, v. 50, no. 12, p. 1209–1222. https://doi.org/10.1139/cjes-2013-0064

Pickett, J., 2018. Method development for the systematic separation of the < 63 mm heavy mineral fraction from bulk till samples; M.Sc. thesis, Queen's University, Kingston, Ontario, 219 p.

Plouffe, A., McClenaghan, M.B., Paulen, R., McMartin, I., Campbell, J., and Spirito, W., 2013. Processing of unconsolidated glacial sediments for the recovery of indicator minerals: protocols used at the Geological Survey of Canada; Geochemistry: Exploration, Environment, Analysis, v. 13, p. 303–313.

Plouffe, A., Ferbey, T., Hashmi, S., and Ward, B., 2016. Till geochemistry and mineralogy: vectoring towards Cu porphyry deposits in British Columbia, Canada; Geochemistry: Exploration, Environment, Analysis, v. 16, no. 3–4, p. 213–232. https://doi.org/10.1144/geochem2015-398

Plouffe, A. and Ferbey, T., 2017. Porphyry Cu indicator minerals in till: a method to discover buried mineralization; *in* Indicator minerals in till and stream sediments of the Canadian Cordillera, (ed.) T. Ferbey, A. Plouffe, and A. Hicken; Mineral Association of Canada, Topics in Mineral Sciences Volume 47 and Geological Association of Canada, Special Paper 50, p. 129–159.

Rennie, D., Friedman, D., Gray, J., Bolu, M., Pozder, S., and Greskovich, G., 2013. Canadian National Instrument 43-101 technical report on the Sisson project, New Brunswick, Canada; Samuel Engineering Inc., 302 p.

Sandmann, D., 2015. Method development in automated mineralogy; Ph.D. thesis, Technischen Universität Bergakademie Freiberg, Freiberg, Germany, 152 p.

Seaman, A.A., 2003. Follow-up till geochemistry, Coldstream (NTS21J/06) map area and part of the adjacent Napadogan (NTS 21J/07) map area, York and Carleton counties, New Brunswick; New Brunswick Department of Natural Resources: Minerals, Policy and Planning Division, Mineral Resource Report 2003-11, 103 p.

Seaman, A.A. and McCoy, S.M., 2008. Multiple Wisconsinian tills in the Sisson Brook exploration trench of Geodex Minerals Ltd., York County, west-central New Brunswick; *in* Geological investigations in New Brunswick for 2007, (ed.) G.L Martin; New Brunswick Department of Natural Resources: Minerals, Policy, and Planning Division, Mineral Resource Report 2008-1, p. 1–34.

Shilts, W.W., 1978. Nature and genesis of mudboils, central Keewatin, Canada; Canadian Journal of Earth Sciences, v. 15, no. 7, p. 1053–1068. https://doi.org/10.1139/e78-113

Simandl, G.J., Mackay, D.A.R., Ma, X., Luck, P., Gravel, J., Grcic, B., and Redfearn, M., 2015. Direct and indirect indicator minerals in exploration for carbonatite and related ore deposits — an orientation survey, British Columbia, Canada; *in* Application of indicator mineral methods to exploration, (co-ord.) M.B. McClenaghan and D. Layton-Matthews; 27th International Applied Geochemistry Symposium, Short Course No. 2, p. 33–39.

Snow, R.J. and Coker, W.B., 1987. Overburden geochemistry related to W-Cu-Mo mineralization at Sisson Brook, New Brunswick, Canada: an example of short-and long-distance glacial dispersal; Journal of Geochemical Exploration, v. 28, no. 1–3, p. 353–368. https://doi.org/10.1016/0375-6742(87)90057-4

Spry, P.G., 1982. An unusual gahnite-forming reaction, Geco base-metal deposit, Manitouwadge, Ontario; The Canadian Mineralogist, v. 20, no. 4, p. 549–553.

Spry, P.G. and Scott, S.D., 1986. The stability of zincian spinels in sulphide systems and their potential as exploration guides for metamorphosed massive sulphide deposits; Economic Geology, v. 81, no. 6, p. 1446–1463. https://doi.org/10.2113/gsecongeo.81.6.1446

Stea, R., Johnson, M., Hanchar, D., Paulen, R., and McMartin, I., 2009. The geometry of kimberlite indicator mineral dispersal fans in Nunavut, Canada; *in* Application of till and stream sediment heavy mineral and geochemical methods to mineral exploration in western and northern Canada, (ed.) I. McMartin and R. Paulen; Geological Association of Canada, GAC Short Course Notes 18, p. 1–13.

Stea, R., Seaman, A., Pronk, T., Parkhill, M., Allard, S., and Utting, D., 2011. The Appalachian glacier complex in Maritime Canada; *in* Quaternary glaciations – extent and Chronology, A Closer Look, (ed.) J. Ehlers and P.L. Gibbard; Elsevier Science Publishers, p. 631–659.

Stoddard, E.F., 1979. Zinc-rich hercynite in high-grade metamorphic rocks: a product of the dehydration of staurolite; American Mineralogist, v. 64, p. 736–741.

Stubley, M. and Irwin, D., 2019. Bedrock geology of the Slave Craton, Northwest Territories and Nunavut; Northwest Territories Geological Survey, Open File 2019-01, digital file.

Sylvester, P.J., 2012. Use of the mineral liberation analyzer (MLA) for mineralogical studies of sediments and sedimentary rocks; *in* Quantitative mineralogy and microanalysis of sediments and sedimentary rocks, (ed.) P. Sylvester; Mineralogical Association of Canada, Short Course Series, v. 42, p. 1–16.

Theart, H.F.J., Ghavami-Riabi, R., Mouri, H., and Gräser, P., 2011. Applying the box plot to the recognition of footwall alteration zones related to VMS deposits in a high-grade metamorphic terrain, South Africa, a lithogeochemical exploration application; Geochemistry, v. 71, no. 2, p. 143–154. https://doi.org/10.1016/j.chemer.2010.09.002

Thomas, A., 1978. Volcanic stratigraphy of the Izok Lake greenstone belt, District of Mackenzie, NWT; Ph.D. thesis, University of Western Ontario, London, Ontario, 220 p.

van Staal, C.R., 1991. Dunnage and Gander zones, New Brunswick: Canadian Appalachian region; New Brunswick Natural Resources and Energy: Minerals, Policy, and Planning Division, Open File Report 91-2, 39 p.

Wentworth, C.K., 1922. A scale of grade and class terms for clastic sediments; The Journal of Geology, v. 30, no. 5, p. 377–392.

Wilton, D.H.C. and Winter, L.S., 2012. SEM-MLA (scanning electron microscope-mineral liberation analyser) research on indicator minerals in till and stream sediments—an example from the exploration for awaruite in Newfoundland and Labrador; *in* Quantitative mineralogy and microanalysis of sediments and sedimentary rocks, (ed.) P. Sylvester; Mineralogical Association of Canada, Short Course Series, v. 42, p. 265–283.

Wilton, D., Thompson, G., and Grant, D., 2017. The use of automated indicator mineral analysis in the search for mineralization – a next generation drift prospecting tool; EXPLORE, v. 174, p. 1–18.

Zaleski, E., Froese, E., and Gordon, T.M., 1991. Metamorphic petrology of Fe-Zn-Mg-Al alteration at the Linda volcanogenic massive sulphide deposit, Snow Lake, Manitoba; The Canadian Mineralogist, v. 29, no. 4, p. 995–1017.

Zhang, W., Lentz, D.R., Thorne, K.G., and McFarlane, C., 2016. Geochemical characteristics of biotite from felsic intrusive rocks around the Sisson Brook W-Mo-Cu deposit, west-central New Brunswick: an indicator of halogen and oxygen fugacity of magmatic systems; Ore Geology Reviews, v. 77, p. 82–96. https://doi.org/10.1016/j.oregeorev.2016.02.004

Zhang, W., McFarlane, C.R.M., and Lentz, D.R., 2013. Mineralogical, petrological, and petrogenetic analysis of felsic intrusive rocks at the Sisson Brook W-Mo-Cu deposit, west-central New Brunswick; Acta Geologica Sinica (English edition), v. 87, p. 831–834.